Parameters, Calculation of Nuclear Magnetic Resonance

Cynthia J. Jameson
University of Illinois at Chicago, Chicago, IL, USA

The fundamental parameters that reproduce a nuclear magnetic resonance (NMR) spectrum in gases, liquids, and solids are the NMR chemical shift of the nucleus, the indirect nuclear spin–spin coupling, and the nuclear quadrupole coupling. All three quantities are tensors whose directional properties are intimately related to the local electronic structure at the nucleus; the third is trivially related to the electric field gradient (EFG) at the nucleus, so we consider the latter. The theoretical methods used in calculating the shielding (which is measured as a chemical shift relative to some convenient reference substance), the J*-coupling, and the EFG are considered here, also the challenges in the accurate calculation of these quantities, including relativistic effects, dynamics, and solid-state effects. The sensitivity to intramolecular geometry, local and long-range environment, and dynamic averaging that make these NMR parameters particularly useful as probes for analysis also provide major challenges in carrying out theoretical calculations.*

1 INTRODUCTION

The fundamental parameters that reproduce an NMR spectrum in gases, liquids, and solids are the NMR chemical shift of the nucleus, the indirect nuclear spin–spin coupling, and the nuclear quadrupole coupling. All three

Update based on the original article by Cynthia J. Jameson, *Encyclopedia of Analytical Chemistry*, © 2000, John Wiley & Sons, Ltd.

Encyclopedia of Analytical Chemistry, Online © 2006–2013 John Wiley & Sons, Ltd.

This article was published in the *Encyclopedia of Analytical Chemistry* in 2013 by John Wiley & Sons, Ltd.
DOI: 10.1002/9780470027318.a6109.pub2

quantities are tensors whose directional properties are intimately related to the local electronic structure at the nucleus. In gases and in liquids where free tumbling of the molecules bearing the nuclear spin leads to isotropic averaging of these quantities, only a single number determines the frequencies in the NMR spectrum: the isotropic average value, the average of three components along the principal axes of the tensor. In the solid state, restricted motion permits the tensors to manifest all the components, whether the sample is a polycrystalline powder, an amorphous solid, or a single crystal.

There is a fourth parameter that is just as important, the direct nuclear spin dipole–dipole interaction, which depends directly and entirely on the third power of the inverse of the distance between two nuclei, whether bonded or otherwise, irrespective of the electronic structure. It is a very important parameter in the solid state because it depends on structure, and for protons in a large molecule in solution, it provides the nuclear Overhauser effect (NOE) that makes it possible to elicit the geometrical structure of the nonfloppy parts of the molecule. This direct dipole–dipole interaction parameter is not considered in the theoretical calculations described here because of the trivial mathematical relationship between the parameter and the direct through-space distance.

1.1 Absolute Shielding Tensor and Nuclear Magnetic Resonance Chemical Shift

The NMR spectrum provides the chemical shift δ relative to a chosen reference substance in a chosen medium. The definition of the chemical shift, usually expressed in parts per million (ppm), is given in Equation (1)

$$\delta \equiv \frac{\nu - \nu_{\mathrm{ref}}}{\nu_{\mathrm{ref}}} \tag{1}$$

where ν is the resonance frequency for the nucleus of interest in the sample and ν_{ref} is the resonance frequency for the reference. The resonance frequency is determined by a fundamental molecular electronic property called the *nuclear magnetic shielding*, $\boldsymbol{\sigma}$, which is defined by the Hamiltonian for the energy of a single nucleus N possessing a nuclear magnetic moment $\boldsymbol{\mu}_{\mathrm{N}}$, in an external magnetic field $\mathbf{B}$, Equation (2) (where Z stands for Zeeman and CS stands for chemical shift).

$$\mathcal{H}_{\mathrm{Z+CS}} = -\boldsymbol{\mu}_{\mathrm{N}} \cdot (1 - \sigma) \cdot \mathbf{B} \tag{2}$$

The magnetic field experienced by the nucleus at its site is different from the applied magnetic field $\mathbf{B}$ because of the small field $\mathbf{B}_{\mathrm{local}}$ arising from the circulations of the electrons induced by the external magnetic field, Equation (3)

$$(\mathbf{B}_{\mathrm{local}})_{\alpha} = (1 - \sigma)_{\alpha\beta}\mathbf{B}_{\beta}, \quad \alpha, \beta = x, y, z \tag{3}$$

thus, Equation (4)

$$\mathcal{H}_{\mathrm{CS}} = +\boldsymbol{\mu}_{\mathrm{N}} \cdot \sigma \cdot \mathbf{B} \tag{4}$$

The term ''magnetic shielding'' implies that the magnetic dipole of a nucleus at that site would be shielded from the full effect of the external field by the influence of the induced electronic motions. For free atoms, $\boldsymbol{\sigma}$ is always positive because this circulation generates a shielding field that opposes the applied field. In a molecule, the presence of other nuclei hinders this circulation to an extent that depends on the electronic distribution and may even lead to a negative $\boldsymbol{\sigma}$. Depending on the symmetry of the electronic distribution at the nuclear site, some of the components $\boldsymbol{\sigma}_{\alpha\beta}$ may be zero or identical. For example, for a linear molecule there are only two unique components, $\boldsymbol{\sigma}_{zz}$ and $\boldsymbol{\sigma}_{xx}$, where z is along the molecular axis; these components are designated as $\boldsymbol{\sigma}_{||}$ and $\boldsymbol{\sigma}_{\perp}$, respectively.

Theoretical calculations of the nuclear magnetic shielding provide the entire shielding tensor $\boldsymbol{\sigma}$ on an absolute basis, that is, with respect to a bare nucleus. The chemical shift δ expresses a difference in nuclear magnetic shielding, Equation (5)

$$\delta \equiv \frac{\nu - \nu_{\mathrm{ref}}}{\nu_{\mathrm{ref}}} = \frac{\sigma_{\mathrm{ref}} - \sigma}{1 - \sigma_{\mathrm{ref}}} \tag{5}$$

Usually, but not always, σ_{ref} can be neglected relative to 1.0, so sometimes it is sufficient to use Equation (6),

$$\delta \approx (\sigma_{\mathrm{ref}} - \sigma) \tag{6}$$

A *negative chemical shift* means that the nucleus located at site A sees a more shielded (smaller) magnetic field than does the nucleus in the reference substance, so that the *applied field has to be made higher* in order to achieve resonance with the nuclear spin energy separation at site A.

We see from Equation (2) that the mathematical terms in the total energy of a molecule that are bilinear in the external homogeneous magnetic field $\mathbf{B}$ and the nuclear magnetic moment $\boldsymbol{\mu}$ determine the nuclear magnetic shielding $\boldsymbol{\sigma}$ for a nucleus in a molecule. The theoretical calculation of NMR chemical shifts from first principles therefore consists of collecting all such bilinear terms in the energy of a molecule in the presence of both an external magnetic field and a nuclear magnetic moment located at the observed site to obtain the absolute

Encyclopedia of Analytical Chemistry, Online © 2006–2013 John Wiley & Sons, Ltd.

This article was published in the *Encyclopedia of Analytical Chemistry* in 2013 by John Wiley & Sons, Ltd.
DOI: 10.1002/9780470027318.a6109.pub2

shielding tensor quantities $\boldsymbol{\sigma}$. A separate calculation is required for the reference molecule. The NMR chemical shift tensor can then be calculated from differences between $\boldsymbol{\sigma}$ and σ_{ref}.

1.2 Indirect Spin–Spin Coupling Tensor

Usually, more than one nuclear spin is present in the observed molecule. The interaction of nuclear spins N and N′ is composed of a direct through-space dipolar coupling (coupling of the bare nuclear magnetic dipole moments) and an indirect interaction by way of the electrons. The Hamiltonian for this interaction energy is, Equation (7)

$$\mathcal{H}_{\mathbf{D}+\mathbf{J}} = \mu_N \cdot (\mathbf{D} + \mathbf{J}) \cdot \mu_{N'} \tag{7}$$

The direct dipolar coupling tensor **D** is symmetric, with the principal components summing to zero (a traceless tensor), and depends entirely on the distance vector between N and N′. In an oriented system, both **D** and **J** (the spin–spin coupling) contribute to the observed spectrum. In a rapidly tumbling molecule in solution, only the isotropic average of **J** survives ($\mathbf{J}_{iso} = (1/3)[\mathbf{J}_{xx} + \mathbf{J}_{yy} + \mathbf{J}_{zz}]$); the anisotropic part averages to zero. A *positive* **J** results from an interaction that minimizes the energy when the two nuclear spins are *antiparallel*. The theoretical calculation of the **J** tensor from first principles consists of collecting all such bilinear terms in the energy of a molecule, as shown in Equation (7).

1.3 Electric Field Gradient Tensor and Nuclear Quadrupole Coupling Constant

All nuclei with spin $I > 1/2$ have an ellipsoidal distribution of charge and an electric quadrupole moment eQ, where e is the magnitude of the charge of an electron. Q is positive if the nucleus is prolate (cigarlike), negative if oblate (pancakelike). Q is an intrinsic property of the nucleus. Energy is minimized by appropriate alignment of an electric quadrupole in an EFG. At a nuclear site in a molecule, there is an EFG when there is an asymmetry in the charge distribution due to the electrons and other nuclei. This EFG is represented by $e\mathbf{q}$. The energy of a nuclear quadrupole is quantized according to its orientation in the EFG, even in the absence of an external magnetic field. The electrostatic energy of interaction between the electric quadrupole moment and the EFG is expressed in terms of the nuclear quadrupole coupling constant ($e^2 Q q_{zz}/\hbar$).

The magnetic dipole moment of a quadrupolar nucleus is along the axis of symmetry of the nuclear charge distribution. Thus, when a quadrupolar nucleus is placed in a magnetic field so that the nuclear magnetic dipole tends to align with the external magnetic field, the interaction of the electric quadrupole with the internal EFG at the nuclear site in the molecule affects the nuclear magnetic energy levels. The tensor coupling between the nuclear spin and the EFG $e\mathbf{q}$ at the nucleus is described by the Hamiltonian, Equation (8)

$$\mathcal{H}_Q = \mathbf{I}_N \cdot \frac{eQ}{2I(2I-1)} e\mathbf{q} \cdot \mathbf{I}_{N'} \tag{8}$$

Similarly to **D**, the EFG tensor is traceless: the isotropic average of energy terms involving **q** is zero. Thus, in liquids or gases, the positions of the lines in the NMR spectrum are not affected by the nuclear quadrupole coupling. In solids, the nuclear quadrupole coupling can dominate the NMR spectrum and measurements of the nuclear quadrupole coupling tensor in single crystals or powders provide the EFG tensors.

1.4 Nuclear Magnetic Resonance Parameters in Gases, Liquids, and Solids

In gases and liquids, isotropic averaging caused by the rapid tumbling of molecules leads to observations of only the isotropic part of $\boldsymbol{\sigma}$ and **J**, which are given by one-third the sum of the principal components of these tensors. At the same time, **D** and **q** being traceless means that this sum is zero. Thus, in liquids or gases, the positions of the lines in the NMR spectrum are not affected by either the direct dipolar coupling or the nuclear quadrupole coupling. To a good approximation, neither the chemical shift nor the spin–spin coupling **J** is dependent of the strength of the magnetic field. Actually, one has to be quite specific in defining the environment of the nucleus in both sample and reference because the NMR chemical shift is very sensitive to these. For example, the chemical shift of a ^{13}C nucleus in molecule A relative to the usual reference is tetramethylsilane (TMS) is $\delta_A = \sigma(^{13}C, \text{in TMS, in } CDCl_3 \text{ solution}, x_A, x_{TMS}, x_{CDCl_3}, 300\,K) - \sigma(^{13}C, \text{in A, in } CDCl_3 \text{ solution}, x_A, x_{TMS}, x_{CDCl_3}, 300\,K)$.

It is important to specify completely all the variables (e.g. mole fractions x_A, etc.) that determine the observed chemical shift because the nuclear magnetic shielding is so sensitive to factors of molecular structure and environment. There is an intrinsic mass and temperature dependence of the chemical shift, the spin–spin coupling, and the nuclear quadrupole coupling because all three are functions of the electron distribution, which in turn is a function of the nuclear positions. As the internuclear separations are weighted according to the vibrational functions, the thermal average values of these NMR parameters are dependent on the vibrational and rotational state populations. Furthermore, all three NMR parameters are dependent on the medium as each one is

Encyclopedia of Analytical Chemistry, Online © 2006–2013 John Wiley & Sons, Ltd.

This article was published in the *Encyclopedia of Analytical Chemistry* in 2013 by John Wiley & Sons, Ltd.
DOI: 10.1002/9780470027318.a6109.pub2

affected by the electronic environment, and the electron distribution is affected by intermolecular interactions and external electric fields. For protons, the medium effects are generally small, whereas they can be quite large for other nuclei.

In oriented molecules, such as in liquid crystal solutions, polycrystalline powders, single crystals, or amorphous powders, the tensor nature of the three NMR parameters manifest themselves in the spectrum. In principle, one can measure both the anisotropy and asymmetry of the **J** tensor in rigid solids. However, the anisotropy of **J** transforms similarly to the direct dipolar coupling, thus the two interactions cannot be easily separated via experiment. The anisotropy in **J** is predicted to become more important for coupling constants involving heavier nuclei, whereas **D** depends only on the internuclear distance. Rapid magic-angle spinning (MAS) can be used to obtain high-resolution spectra of solids by removing the effects of the anisotropic terms, which in general have a $P_2(cos\theta)$ dependence. The angle for which $(3cos^2\theta - 1)$ equals zero is the magic angle 54.74°. The terms that give rise to the NMR spectrum of quadrupolar nuclei include, in addition, a $P_4(cos\theta)$ dependence. Various techniques have been used to determine these three NMR tensors individually by experiment, including the orientations of their principal axis systems. In solids, the spinning sidebands observed in slow MAS NMR spectra arising from tightly **J**-coupled spin pairs contain valuable information about NMR parameters such as the orientation of chemical shift tensors and the sign of **J**. Multidimensional NMR spectra in solids permit the separate determination of the isotropic chemical shifts and the anisotropic line shapes that contain chemical shift tensor and quadrupole coupling information for each site.

Thus, we have seen that the parameters of an NMR spectrum are related to fundamental molecular electronic properties: the chemical shift is related to nuclear magnetic shielding $\boldsymbol{\sigma}$ and the nuclear quadrupole coupling is related to the EFG tensor $e\mathbf{q}$. The indirect spin–spin coupling **J** is itself a molecular electronic property. Therefore, the general approach to the theoretical calculations of these NMR parameters is through a quantum mechanical calculation of molecular electronic properties in the isolated molecule. Any medium effects that have to be included, when they are large enough, require, in addition, ensemble averages for a gas, liquid, or solution. The calculation of the EFG is simplest, as this is a property of the unperturbed electronic state of the molecule. Since $\boldsymbol{\sigma}$ and **J** are electronic properties associated with the presence of magnetic fields and fields generated by nuclear magnetic moments, their calculation requires the general approaches that apply to multiple perturbations. Furthermore, as the probe nucleus senses electronic environments in the immediate vicinity of the nucleus, high-level calculations that take into account electron correlation have to be used for all three parameters to achieve accuracy, and relativistic corrections are sometimes necessary. Density functional methods have been very successful and can compete favorably with *ab initio* calculations.

2 GENERAL THEORETICAL METHODS

The mechanisms by which a nuclear magnetic moment interacts with the molecular field and with external magnetic or electric fields in the ground vibronic state were originally articulated in fundamental work by Ramsey.[1–3] For a unified approach to molecular electronic properties, which explicitly shows where the contributing terms arise and thereby also permits the relationships between electronic properties to be perceived, the reader is referred to the articles by Michelot.[4,5] The complete molecular Hamiltonian in the presence of external magnetic and electric fields, including all relevant interaction terms involving nuclear magnetic moments (such as interaction between the nuclear magnetic moment and the field induced at the nucleus by the molecular motion, as well as those related to the interaction of the magnetic moment induced by this molecular motion with an external magnetic field), treats electrons and nuclei as Dirac particles. Relativistic effects are included from the beginning and effects due to the finite dimensions of nuclei are also taken into account, so that the nuclear quadrupole coupling is a natural outcome.[4] Using this Hamiltonian with relativistic corrections for a free molecule in a nondegenerate electronic state, a second-order calculation in degenerate perturbation theory leads to the explicit expressions for the contributing terms to nuclear magnetic shielding $\boldsymbol{\sigma}$, indirect spin–spin coupling **J**, nuclear electric quadrupole coupling, and all other molecular electronic properties.[5]

2.1 Multiple Perturbation Theory

All the terms in the molecular Hamiltonian given by Michelot[4] may be treated as perturbations added to a zeroth-order part (the kinetic energy of the electrons together with the total coulomb potential energy of all the electrons and nuclei, assumed to have already been solved). These include terms bilinear in $\boldsymbol{\mu}_N$ and **B**. In first order, these lead to energy terms that are of the form given by Equation (4), providing the formal expression for the so-called diamagnetic part of the nuclear magnetic shielding $\boldsymbol{\sigma}$. In second order, the terms in the molecular Hamiltonian that are linear in $\boldsymbol{\mu}_N$ together with those

Encyclopedia of Analytical Chemistry, Online © 2006–2013 John Wiley & Sons, Ltd.

This article was published in the *Encyclopedia of Analytical Chemistry* in 2013 by John Wiley & Sons, Ltd.
DOI: 10.1002/9780470027318.a6109.pub2

linear in **B** lead to energy terms that are also of the form given by Equation (4), providing the formal expression for the so-called paramagnetic part of the nuclear magnetic shielding **σ**. Michelot's expression[5] derived for nuclear magnetic shielding **σ** reduces to that given by Ramsey[1,2] if the origin of the molecular frame is placed at the center of the nucleus of interest, the orientation being that of the Eckart frame. Formally, the shielding term for nucleus N is given by Equation (9):

$$\begin{aligned}\sigma_{\alpha\beta}(\mathrm{N}) =& \frac{\mu_0 e^2}{8\pi m}\langle 0|\sum_k \{(r_{k\mathrm{N}} r_{k0}) r_{k\mathrm{N}}{}^{-3}\delta_{\alpha\beta} \\ & - (r^{\alpha}_{k\mathrm{N}} r^{\beta}_{k0}) r_{k\mathrm{N}}{}^{-3}\}|0\rangle - \frac{\mu_0 e^2}{8\pi m^2}\sum_{n\neq 0}({}^1E_n - E_0)^{-1} \\ & \times \{\langle 0|\sum_k r_{k\mathrm{N}}{}^{-3} L^{\alpha}_{k\mathrm{N}}|n\rangle\langle n|\sum_j L^{\beta}_{j0}|0\rangle \\ & + \langle 0|\sum_j L^{\beta}_{j0}|n\rangle\langle n|\sum_k r_{k\mathrm{N}}{}^{-3} L^{\alpha}_{k\mathrm{N}}|0\rangle\} \end{aligned} \quad (9)$$

The first index $\alpha(=x,y,z)$ is associated with the nuclear magnetic moment and the second index $\beta(=x,y,z)$ is associated with the external magnetic field. L^{β}_{j0} is the β component of the orbital angular momentum operator for the *j*th electron with respect to the chosen origin (the so-called gauge origin) and $\boldsymbol{r}_{k0}$ is the distance vector between the *k*th electron and the origin. $L^{\alpha}_{k\mathrm{N}}$ is the α component of the orbital angular momentum operator for the *k*th electron with respect to the nucleus N as origin. $\boldsymbol{r}_{k\mathrm{N}}$ is the distance vector between the *k*th electron and the nucleus N. *m* and *e* are the mass and charge of the electron, μ_0 is the magnetic permeability of a vacuum. *E* stands for the energy at states 0 and *n* (0 is the lowest state and *n* is an index that runs through all the states of the molecule). In Equation (9), the second term in the expression for $\boldsymbol{\sigma}_{\alpha\beta}(\mathrm{N})$, the paramagnetic term, is written in the so-called sum over states (SOS) form, that is, in terms of the sum $\sum_n$ over all excited states designated by the symbol $|n\rangle$. In the symbol $\langle 0|\sum_k r_{k\mathrm{N}}{}^{-3} L^{\alpha}_{k\mathrm{N}}|n\rangle$, the operators for the angular momentum and the distance vector for the electrons are integrated over the ground state $\langle 0|$ and the excited state $|n\rangle$.

In the same way, the terms in the molecular Hamiltonian that are bilinear in $\boldsymbol{\mu}_{\mathrm{N}}$ and $\boldsymbol{\mu}_{\mathrm{N}'}$ lead to the energy terms that are already of the form given by Equation (7) give rise to the first order part of the indirect spin–spin coupling **J**, usually denoted by $\mathbf{J}^{(1a)}$. The terms linear in $\boldsymbol{\mu}_{\mathrm{N}}$ in the molecular Hamiltonian in the nonrelativistic limit are three, labeled *orbital*, *spin dipolar* (SD), and *Fermi contact* (FC). In second order, products of these lead to various contributions to the spin–spin coupling **J**. The product of orbital terms leads to $\mathbf{J}^{(1b)}$; $\mathbf{J}^{(1a)}$ is sometimes called the *diamagnetic orbital* (OD) contribution or $\mathbf{J}^{(\mathrm{OD})}$, and $\mathbf{J}^{(1b)}$ the paramagnetic orbital (OP) contribution or $\mathbf{J}^{(\mathrm{OP})}$ because of the analogy with the diamagnetic and paramagnetic parts of the shielding tensor. The product of the SD terms leads to $\mathbf{J}^{(2)}$ or $\mathbf{J}^{(\mathrm{SD})}$, and the product of the FC terms leads to $\mathbf{J}^{(3)}$ or $\mathbf{J}^{(\mathrm{FC})}$. By symmetry, there is only one nonvanishing cross-term, resulting from the product of the SD and the contact terms, referred to as $\mathbf{J}^{(4)}$. $\mathbf{J}^{(\mathrm{FC})}$ is purely scalar (isotropic), whereas the others are anisotropic. The motional average of $\mathbf{J}^{(4)}$ is zero, thus, all but $\mathbf{J}^{(4)}$ contribute to the observed isotropic average spin–spin coupling for a rapidly tumbling molecule in solution. All terms contribute to the observed NMR spectrum in solids. The formal expressions for spin–spin coupling in the nonrelativistic limit are shown below in terms of the spin ($\mathbf{S}_k$) and orbital ($L^{\alpha}_{k\mathrm{N}}$) angular momentum of the (*k*th) electron, Equations (10)–(14):

$$\begin{aligned}\mathbf{J}^{(1a)}_{\alpha\beta} =& \frac{2m}{h}\mu_{\mathrm{B}}^2\left(\frac{\mu_0}{4\pi}\right)^2\gamma_{\mathrm{N}}\gamma_{\mathrm{N}'}\langle 0|\sum_k r_{k\mathrm{N}}{}^{-3} r_{k\mathrm{N}'}{}^{-3} \\ & \times [(r_{k\mathrm{N}} r_{k\mathrm{N}'})\delta_{\alpha\beta} - r^{\alpha}_{k\mathrm{N}} r^{\beta}_{k\mathrm{N}'}]|0\rangle \end{aligned} \quad (10)$$

$$\begin{aligned}\mathbf{J}^{(1b)}_{\alpha\beta} =& \frac{1}{h}(2\mu_{\mathrm{B}})^2\left(\frac{\mu_0}{4\pi}\right)^2\gamma_{\mathrm{N}}\gamma_{\mathrm{N}'}\sum_n ({}^1E_n - E_0)^{-1} \\ & \times \left\{\langle 0|\sum_k r_{k\mathrm{N}}{}^{-3} L^{\alpha}_{k\mathrm{N}}|n\rangle \right. \\ & \left. \times \langle n|\sum_j r_{j\mathrm{N}'}{}^{-3} L^{\beta}_{j\mathrm{N}'}|0\rangle + \mathrm{cc}\right\} \end{aligned} \quad (11)$$

$$\begin{aligned}\mathbf{J}^{(2)}_{\alpha\beta} =& -\frac{1}{h}(2\mu_{\mathrm{B}}\hbar)^2\left(\frac{\mu_0}{4\pi}\right)^2\gamma_{\mathrm{N}}\gamma_{\mathrm{N}'}\sum_n ({}^3E_n - E_0)^{-1} \\ & \times \left\{\langle 0|\sum_k 3 r_{k\mathrm{N}}{}^{-5}\left(\mathbf{S}_k \mathbf{r}_{k\mathrm{N}}\right) r^{\alpha}{}_{k\mathrm{N}} - r_{k\mathrm{N}}{}^{-3}\mathbf{S}^{\alpha}_k|n\rangle \right. \\ & \left. \times \langle n|\sum_j 3 r_{j\mathrm{N}'}{}^{-5}\left(\mathbf{S}_k \mathbf{r}_{j\mathrm{N}'}\right) r^{\beta}_{j\mathrm{N}'} - r_{j\mathrm{N}'}{}^{-3}\mathbf{S}^{\beta}_j|0\rangle + \mathrm{cc}\right\} \end{aligned} \quad (12)$$

$$\begin{aligned}\mathbf{J}^{(3)}_{\alpha\beta} =& -\frac{1}{h}\left(\frac{16\pi\mu_{\mathrm{B}}\hbar}{3}\right)^2\left(\frac{\mu_0}{4\pi}\right)^2\gamma_{\mathrm{N}}\gamma_{\mathrm{N}'} \\ & \times \sum_n ({}^3E_n - E_0)^{-1}\left\{\langle 0|\sum_k \delta\left(r_{k\mathrm{N}}\right)\mathbf{S}^{\alpha}_k|n\rangle \right. \\ & \left. \times \langle n|\sum_j \delta\left(r_{j\mathrm{N}'}\right)\mathbf{S}^{\beta}_j|0\rangle + \mathrm{cc}\right\} \end{aligned} \quad (13)$$

Encyclopedia of Analytical Chemistry, Online © 2006–2013 John Wiley & Sons, Ltd.

This article was published in the *Encyclopedia of Analytical Chemistry* in 2013 by John Wiley & Sons, Ltd.
DOI: 10.1002/9780470027318.a6109.pub2

$$\mathbf{J}^{(4)}_{\alpha\beta} = -\frac{2}{h}\frac{16\pi\mu_B\hbar}{3}2\mu_B\hbar\left(\frac{\mu_0}{4\pi}\right)^2\gamma_N\gamma_{N'} \times \sum_n ({}^3E_n - E_0)^{-1}\left\{\langle 0|\sum_k \delta\left(r_{kN}\right)\mathbf{S}^{\alpha}_k|n\rangle \times \langle n|\sum_j 3r_{jN'}{}^{-5}\left(\mathbf{S}_k r_{jN'}\right)r^{\beta}_{jN'} - r_{jN'}{}^{-3}\mathbf{S}^{\beta}_j|0\rangle + \text{cc}\right\} \quad (14)$$

where cc indicates the conjugate term in which the two operators are switched. μ_B is the Bohr magneton, γ_N is the magnetogyric ratio for the nucleus N. $\delta(\boldsymbol{r}_{kN})$ is the Dirac delta function which picks out the value at $\boldsymbol{r}_{kN} = 0$ in any integration over the coordinates of the kth electron.

The coupling contributions $\mathbf{J}^{(1a)}$ or $\mathbf{J}^{(OD)}$ and $\mathbf{J}^{(1b)}$ or $\mathbf{J}^{(OP)}$ can be thought of as arising through paramagnetic and diamagnetic currents induced in the molecular electronic distribution by the nuclear magnetic moment of one of the nuclei and coupling to the magnetic moment of the other nucleus. The coupling contribution $\mathbf{J}^{(3)}$ or $\mathbf{J}^{(FC)}$ can be considered as arising from the transmission of spin information from nuclear spin to electron spin. Owing to the finite density of the electron at the nucleus, this information is passed on through the spin interaction between electrons in the molecule and transmitted at the other end via electron spin density at the other nucleus. The dipole–dipole interaction between the nuclear and electron spins lead to the coupling contribution $\mathbf{J}^{(2)}$ or $\mathbf{J}^{(SD)}$.

The expressions shown here in Equations (9)–(14) are cast in the form of sums over excited states, as they were originally cast in the Ramsey formulation. However, practical calculations are not actually carried out in this form for several reasons. Multiple perturbation theory is more conveniently carried out by using directly the first-order perturbed wavefunction or the first-order density matrix. In other words, for the multiple perturbation of the external magnetic field and the nuclear magnetic moment, the nuclear magnetic shielding may be calculated by first calculating the first-order density matrix of the molecule in the external magnetic field alone, using the operator $\sum_j L^{\beta}_{j0}$, and with this the integrals that account for the second perturbation imposed by the nuclear magnetic moment are then evaluated, using the operator $\sum_k r_{kN}{}^{-3}L^{\alpha}_{kN}$. Or, independently, one could first find the first-order density matrix of the molecule in the presence of the nuclear magnetic moment alone, and with this, evaluate the integrals that account for the second perturbation imposed by the external magnetic field. A physical interpretation is that the nuclear magnetic shielding arises from the interaction of the magnetic moment of the nucleus with the magnetic field due to the current density induced by the external magnet or, equivalently, from the interaction of the current density induced by the nuclear magnetic moment with the external magnetic field. The most common approach is to construct first the electronic response induced by the external magnet and then study its interaction with various nuclei in the molecule. In current practice, the shielding and the **J** coupling are evaluated as derivatives of the electronic energy with respect to the magnetic field and with respect to the nuclear magnetic moments, which permits the use of efficient techniques that have been developed wherein the derivatives are calculated directly from analytically derived expressions, the so-called analytic gradient or analytic derivative approach.

Note that written in the form of Equation (9), the diamagnetic part of the shielding is very easy to calculate, as it requires an average over the electronic ground-state function only. On the other hand, the second-order term, that is, the paramagnetic contribution, requires knowledge of how the presence of the external magnetic field changes the electronic wavefunction of the molecule and the integration requires that this knowledge be especially accurate in the immediate vicinity of the nucleus of interest.

The calculation of the EFG tensor does not require a perturbation treatment as this is one of those electronic properties that can be calculated as an average over the electronic ground-state wavefunction. The zz component of the EFG tensor is given by Equation (15).

$$q_{zz} = \sum_j e_j(3z_j{}^2 - r_j{}^2)r_j^{-5} \quad (15)$$

where e_j is the charge of the jth particle (the electrons, other nuclei, external charges) in the system and the z axis is in the nuclear-fixed coordinate system, that is along the nuclear axis of spin. The spin axis of the nucleus is allowed to rotate with respect to the laboratory frame of reference and the nuclear wavefunction is a product of the intrinsic $\Psi_{\text{intrinsic}}$ and orientation $\Psi_{I,M}$ functions for spin angular momentum described by quantum numbers I and M, Equation (16).

$$\Psi_{\text{total}} = \Psi_{I,M}\Psi_{\text{intrinsic}}\Phi \text{ (electrons other, nuclei, external charges)} \quad (16)$$

For a nucleus in a molecule oriented in the laboratory framework, the components of the field gradient tensor are q_{XX}, q_{YY}, q_{ZZ}. The principal field gradient tensor component q_{zz} for the nucleus in the molecule is related to the laboratory values through the direction cosines between the axes, as follows, Equation (17):

$$q_{zz} = (C_{Xz})^2 q_{XX} + (C_{Yz})^2 q_{YY} + (C_{Zz})^2 q_{ZZ} \quad (17)$$

Encyclopedia of Analytical Chemistry, Online © 2006–2013 John Wiley & Sons, Ltd.

This article was published in the *Encyclopedia of Analytical Chemistry* in 2013 by John Wiley & Sons, Ltd.
DOI: 10.1002/9780470027318.a6109.pub2

In the absence of a magnetic field, the energy of a quadrupolar nucleus in the EFG can be obtained by averaging the electric quadrupole charge over the wavefunction $\Psi_{\text{intrinsic}}$, averaging the squares of the direction cosines over $\Psi_{I,M}$, and averaging $q_{ZZ} = \sum_j e_j(3Z_j^2 - r_j^2)r_j^{-5}$ over the wavefunction Φ (electrons, other nuclei, external charges) expressed in the laboratory frame. The average of the direction cosines over $\Psi_{I,M}$ leads to an energy expression that is proportional to $[3M^2 - I(I+1)]$ in the absence of a magnetic field.

In the presence of a magnetic field, the magnetic dipole moment of a quadrupolar nucleus, which lies along the axis of symmetry of the cigarlike or pancakelike nuclear charge distribution, interacts with the magnetic field. Thus, when a single quadrupolar nucleus in a molecule is placed in a magnetic field, the interaction of the electric quadrupole with the internal EFG at the nuclear site in the molecule leads to a series of $2I$ resonance lines. Thus, a spin $I = 1$ nucleus in an axially symmetric EFG gives a pair of lines separated by $[e^2 q_{ZZ} Q](3/2)$ or more explicitly, by $[e^2 q_{zz} Q](3/2)(3cos^2\theta - 1)/2$, where θ is the angle that the principal symmetry axis of the EFG makes with the external magnetic field. The pair of lines is centered at a frequency that provides the shielding tensor. Both the shielding tensor and the EFG tensor in the *XYZ* (i.e. the laboratory-fixed) coordinate system can be obtained from an oriented molecule in the solid state. Equation (17) permits the determination of the tensor in the *xyz* (i.e. the molecule-fixed) coordinate frame system. Since the EFG is a traceless tensor, the isotropic average is zero. Thus, in the liquid phase the positions of the lines in the NMR spectrum are not affected by the nuclear quadrupole coupling, although information about the latter can still be obtained from quadrupolar relaxation times.

Theoretical calculations of the EFG tensor in *the molecular frame* of an isolated molecule involves evaluating the quantum mechanical average of the operator $q_{zz} = \sum_j e_j(3z_j^2 - r_j^2)r_j^{-5}$ over the ground-state electronic wavefunction for the molecule, where j runs over all electrons and the origin is set at the nucleus in question. To this electronic contribution must be added the nuclear contribution, by evaluating a similar algebraic expression in which e_j are the charges of the other nuclei and z_j and r_j are their positions in the molecular framework with the origin at the nucleus in question. For molecules in a liquid, EFG contributions from neighbors have to be included, which may require a quantum mechanical average or an approximate sum over fixed partial charges.

Reference 6 is a valuable resource.

2.2 Gauge Origin Problem in Calculations of Chemical Shift

In deriving the expressions shown here, the external magnetic field **B** itself does not appear in the Hamiltonian. What appears instead are the magnetic vector potentials associated with the magnetic fields, Equation (18):

$$\mathbf{B} = \nabla \times \mathbf{A} \tag{18}$$

where ∇ is the gradient vector, that is, $B_z = (\partial A_y/\partial x) - (\partial A_x/\partial y)$, for one component. While **B** is determined uniquely if **A** is given, there is, unfortunately, an ambiguity because there is no unique **A** that produces a given **B**. Any transformation that takes a particular **A** into another functional form that also reproduces the same **B** when Equation (18) is applied is called a *gauge transformation*. A mere translation of the origin of the coordinate system can do this transformation; therefore, the set of problems associated with this ambiguity is called the *gauge origin problem*. Physically, there should be no problem at all, as an arbitrary choice of coordinate system should not affect an observable property. Similarly, theoretically there should be no problem at all; any physical quantities resulting from any calculations involving **A** or **B** or physical quantities related to them must be gauge invariant, provided the calculations are done exactly. In fact, calculations are not usually done exactly when one uses an incomplete set of basis functions in which to do the calculations. It has been shown that if the Hartree–Fock equations are solved exactly (which is only possible in the limit of a complete basis) the total current density is gauge independent, as is the nuclear magnetic shielding $\boldsymbol{\sigma}$, while the two parts which are usually called the ''diamagnetic'' and ''paramagnetic'' contributions in Equation (18) are not individually gauge invariant. In practice, calculations are not carried out in the Hartree–Fock limit, so the results of such calculations are not gauge invariant. When a single origin is chosen common to all electrons in the molecule in the definition of $\sum_j L_{j0}^{\beta}$ (and $\boldsymbol{r}_{j0}$), the method is the so-called ''*common origin*'' coupled Hartree–Fock method.

Consider an isolated atom. The external magnetic field induces a current density. The current density vector is orthogonal to the magnetic field vector **B** and to the position vector $\boldsymbol{r}_j$. For a magnetic field in the z direction the current density vectors lie in planes parallel to the xy plane, following the tangents of concentric circles. Here, the natural choice of origin is the position of the nucleus; this leads to a vanishing paramagnetic current density. The current density is entirely the diamagnetic part and corresponds to a local field that opposes the

Encyclopedia of Analytical Chemistry, Online © 2006–2013 John Wiley & Sons, Ltd.

This article was published in the *Encyclopedia of Analytical Chemistry* in 2013 by John Wiley & Sons, Ltd.
DOI: 10.1002/9780470027318.a6109.pub2

external field **B**. Moving the origin off-center to a position other than that of theof the nucleus would make the two parts more difficult to evaluate, but the sum should still be the same as before, so there is no reason to adopt an alternative origin. In molecules, however, there is no choice of origin that can make the paramagnetic part vanish. Changing the location of the origin, in the definition of $\boldsymbol{r}_{j0}$ and $\sum_j L_{j0}^{\beta}$ in Equation (18) leads to differing amounts of positive and negative terms. The worst choice gives very large not quite canceling terms. Clearly, the inner shell electrons in a molecule behave the way they do in the free atom, so that it makes sense to choose the nucleus as the origin when calculating integrals over orbitals centered on that atom. However, that same origin would be a bad choice for orbitals centered on another atom, whereas choosing the nucleus of that atom as origin would present a favorable atomlike calculation for its own inner electrons. Thus, it becomes clear that in order to avoid calculating large positive and negative terms that imperfectly cancel in a single-origin method, some method of using distributed origins would present a practical advantage in computing nuclear magnetic shielding for nuclei in molecules.

The theoretical calculations of nuclear magnetic shielding did not become generally practical even for very small molecules until (i) various ways of using distributed origins were devised and (ii) efficient algorithms for evaluating second-order properties were developed. The various schemes for using distributed origins are known by the acronyms LORG (localized orbital/local origin),[7] IGLO (individual gauge for localized orbitals),[8] GIAOs (gauge-including atomic orbitals),[9] and IGAIM (individual gauges for atoms in molecules).[10] The success of distributed origins comes from the avoidance of calculating large imperfectly canceling contributions. In the first two methods, gauge factors are applied to localized molecular orbitals instead of every atomic orbital. The LORG and IGLO methods introduce an approximation in the form of the closure relation and LORG uses commutation rules and identities. Both have been very successful, although there is the problem of lack of uniqueness in the localization method used. The GIAO method uses gauge factors on every atomic orbital. Although this method of distributed origins had been introduced much earlier than all the others, it was not until the efficient implementation by Peter Pulay using the analytic gradients approach that it became widely successful. The convergence of calculated $\boldsymbol{\sigma}$ values with increasing quality of basis set employed appears to be faster with the GIAO method. GIAOs (sometimes called London orbitals) constitute a physically motivated, compact basis set for magnetic calculations. The field-dependent exponential factor in the London orbital depends on the origin of the coordinate system. A displacement of the origin changes the phase factor of an orbital centered on a nucleus by a factor that is independent of the electronic coordinates. Thus, the calculated properties such as shielding remain unaffected and methods based on the use of such orbitals are gauge invariant. The most important property of the GIAO method is not this formal translational invariance but that the GIAO (the atomic orbital multiplied by the gauge factor) itself represents to first order the eigenfunctions of a one-electron system that has been perturbed by an external magnetic field. GIAOs thus incorporate the bulk of the effect of the magnetic field at the basis function level. The IGAIM approach amounts to constructing the induced current density distribution of a molecule from its constituent atoms, following the highly successful atoms-in-molecules concepts of R.F.W. Bader. It differs from LORG, IGLO, and GIAO in that the gauge origins are determined by properties of the charge density in real space rather than by the behavior exhibited by the basis functions in the Hilbert space of the molecular wavefunction. All these distributed origin methods (GIAO, IGLO, LORG, IGAIM) and any single common origin method should lead to identical results at the Hartree–Fock level in the limit of a complete set of basis functions. The differences lie in the rate of convergence as the number of basis functions is increased. The various distributed-origins methods converge toward the Hartree–Fock limit faster than while using a single origin. Common origin calculations require much larger basis sets to provide nearly origin-independent results comparable to the results from distributed-origin methods.

The use of GIAO orbitals for calculating magnetic properties involving an external magnetic field is now standard in many software packages for routine calculations of shielding and is usually preferred to other procedures for imposing gauge–origin independence.

2.3 Challenges in Calculations of Spin–Spin Coupling

There are no gauge problems in spin–spin coupling calculations; as seen in Equations (10)–(14), only operators with their origin at the nucleus ($r_{k\mathrm{N}}$ and $r_{k\mathrm{N}}{}^{-3}L_{k\mathrm{N}}^{\alpha}$) appear. The calculations of spin–spin coupling have their own associated challenges. As can be seen in Equations (10)–(14), the nature of some of the indirect spin–spin coupling mechanisms requires calculations with uncoupled spin states. Thus, the spin-unrestricted approaches that are normally applied to open shell systems have to be used, otherwise the poor description of triplet excitations give rise to large errors. When there is a nonsinglet ground state with lower energy than the restricted Hartree–Fock singlet ground state, the calculations of the $\mathbf{J}^{(\mathrm{SD})}$ and $\mathbf{J}^{(\mathrm{FC})}$ terms require

Encyclopedia of Analytical Chemistry, Online © 2006–2013 John Wiley & Sons, Ltd.

This article was published in the *Encyclopedia of Analytical Chemistry* in 2013 by John Wiley & Sons, Ltd.
DOI: 10.1002/9780470027318.a6109.pub2

higher order calculations than the self-consistent field (SCF). The Coupled cluster (CC) theory at CCSD (coupled cluster singles and doubles) level leads to much improved accuracy, although instabilities occur at CCSD(T) (coupled cluster singles and doubles with some triple excitations) level and one needs to go further, to CC3, to avoid them. Furthermore, the usually (not always) dominant FC contribution in Equation (13) requires that the spin densities are highly accurate at the location of the nucleus, and this is not easily achieved when the basis functions used are the standard Gaussian form, having no cusp at the nucleus. This requires that basis set augmentation functions with tight (steep) exponents be added to the uncontracted basis sets, which are subsequently recontracted. On the other hand, the OP term has a linear dependence on momentum, which indicates the importance of the addition of more diffuse functions to the basis. The SD, OD, and OP terms are of importance when considering the anisotropy of the **J** tensor. In particular, the cross-term between SD and FC is known to dominate the anisotropy of one-bond **J**. For molecules containing atoms no heavier than carbon, the FC contribution is generally the largest term. It comprises almost the entire coupling – especially for the molecules involving only single bonds. One-bond **J** (in particular the FC component) has a very strong dependence on internuclear distance, thus vibrational averaging is important for accurate calculations. At present, the state of the theory is not yet at the level where, unlike chemical shifts, the most accurate calculations are about the same level of accuracy as the experimental values.

Relativistic effects influence spin–spin couplings much earlier (at lower atomic numbers) than other properties, owing to the strong dependence of **J** on the electronic structure at the position of the nucleus and its immediate vicinity. In fact, Equations (10)–(14) are valid only for the point nucleus in the nonrelativistic limit. For heavy nuclei, it is necessary to start out with the relativistic treatment described in Section 2.6, as the nonrelativistic theory may lead to unrealistic calculated values.[11] In relativistic theory, the indirect spin–spin coupling constant does not partition into the same terms as in Equations (10)–(14).

2.4 *Ab Initio* Methods

In this section, we consider approaches to the calculation of NMR parameters from electronic structure theory from an approximate electronic wavefunction. In the next section, we consider calculations of these parameters from an approximate electronic density using density functional theory (DFT). *Ab initio* methods of quantum chemistry are routinely applied to the study of molecular electronic properties, particularly those properties that are associated with molecular spectra, such as NMR spectra. Indeed, widely available electronic structure calculation software packages have become an important tool for NMR spectroscopists for characterization and analysis. Even so, in *ab initio* calculations of NMR parameters using wavefunctions, there are several things that have to be considered: (i) the level of theory that is used (without, with some, or with substantial electron correlation, with or without relativistic corrections), (ii) the set of basis functions. In addition, (iii) the desired degree of averaging over molecular configurations (with or without rovibrational averaging, with or without medium effects), (iv) the availability of tensor data, and (v) the availability of absolute shielding test data in the case of chemical shifts, also have to be considered. In the case of spin–spin coupling, there is very limited information beyond that of the isotropic average values obtained in solution. Only in rare cases is there anisotropy information, so that the only viable additional tests are those of isotropic effects on spin–spin coupling. In the case of ^{13}C chemical shifts, the amount of detailed tensor information from single crystals and polycrystalline powders is so rich that the level of theory, and size of basis sets needed, and the accuracy of geometrical structure data required to achieve agreement with experiment has been established (by D. M. Grant and associates) for a large variety of carbon site types. The level of theory used in *ab initio* calculations of NMR parameters had to improve continuously with the challenges posed by attempts to match experimental results for specific small molecules, as we shall see below (Section 3.1). Here, as opposed to the DFT method, the progression of steps for systematic improvement toward increasing accuracy of the electronic description is well established. A review of the evaluation of NMR parameters from the various standard *ab initio* models, providing the basic equations needed for the calculation of magnetic properties in each case, with computational aspects related to the practical application of each, is available from Helgaker et al.[12] They examine and compare the different methods systematically, analyzing their relative merits and deficiencies. The quality of the results is determined by the level of theory chosen for the calculation: Hartree–Fock (HF or SCF) is for a single electronic configuration, multiconfiguration self-consistent field (MCSCF) for a subset of configurations; there are various levels in the hierarchy of perturbation theory improvements to the Hartree–Fock model (the Møller–Plesset (MP) theory at various orders, MP2, MP3, etc.), as also in polarization propagator methods [random phase approximation (RPA), second-order polarization propagator approximation (SOPPA)], and various levels in the hierarchy of the CC approach (CCSD with singles and doubles, CCSDT, etc.). The ultimate method, the

Encyclopedia of Analytical Chemistry, Online © 2006–2013 John Wiley & Sons, Ltd.

This article was published in the *Encyclopedia of Analytical Chemistry* in 2013 by John Wiley & Sons, Ltd.
DOI: 10.1002/9780470027318.a6109.pub2

full configuration interaction (FCI) can be used only for extremely few (2–6) electrons.

The Hartree–Fock and RPA represent the first level of calculation and are the same approximation for frequency-independent properties such as NMR parameters. Calculations beyond this level are necessary when electron correlation contributions are significant. Since moving up to the next level of theory can become expensive, when calculating NMR parameters for a set of systems, it is prudent to estimate the magnitude of the corrections needed to improve the accuracy. A calculation to estimate the importance of electron correlation to the nuclear shielding should be done. The involvement of multiple bonds or presence of lone pairs at the nucleus of interest is usually an indication that correlated methods have to be used. Furthermore, an estimate of the magnitude of the effects of averaging over molecular configurations is needed in order to determine whether it is sufficient to do a calculation for a single molecule at a fixed geometry in a vacuum. An estimate of the magnitude of relativistic effects on shielding is needed when next neighbors are heavy atoms (particularly halogen atoms), or when the NMR nucleus is a heavy nucleus.

In the finite field method, the NMR parameter (e.g. $\mathbf{J}$) is obtained by differentiating the energy in the presence of the nuclear magnetic moments (or in the presence of the nuclear moment and the external magnetic field for $\boldsymbol{\sigma}$) with respect to the nuclear moments (or with respect to the nuclear moment and the external field for $\boldsymbol{\sigma}$). The addition of a finite field to the total energy expression is a simple extension of existing computer codes for electronic structure calculations and is one of the standard methods for calculating higher order molecular electronic properties such as the nonlinear polarizabilities, for example. Thus, the finite field method is easily used, without additional theoretical development, to study the effects of electron correlation on properties. The drawback is that a finite field calculation has to be carried out for each tensor component of the property. Thus, while the purely isotropic FC term of $\mathbf{J}$ is easily calculated with finite field methods at various levels such as many body perturbation theory (nth order term) (MBPT(n)) and CC methods, the tensor types of mechanisms given in Equations (10)–(12) and (14) require several calculations to yield the various xx, xy, xz, yy, zz, components. On the other hand, direct methods such as the polarization propagator method use analytic expressions that provide all components of the tensor with one calculation. Pulay introduced analytic derivative theory into shielding calculations as a natural extension of his pioneering work in *ab initio* calculations of force constants and equilibrium geometries. In an MBPT(n) calculation, or alternatively the MP nth-order term (MPn) perturbation series, all energy contributions less than or equal to order n in perturbation theory are included. On the other hand, CC methods, in addition to being consistent to a particular order in perturbation theory, include certain classes of energy contributions summed to infinite order. The same kind of infinite summations are also included in polarization propagator methods (RPA, SOPPA, etc.). Thus, SOPPA is not equivalent to the MBPT(2) (second-order MBPT) or MP2 (MP second-order term) level of approximation. The CC approach, by construction, guarantees a hierarchical expansion converging to the FCI limit. Consequently, CC calculations provide a benchmark against which other more cost-effective methods (e.g. DFT methods) are measured and validated. The CC reference state including singles and doubles excitations (CCSD) and triples (CCSD(T) or CCSD-T) has been introduced in shielding calculations by Gauss; CC has been used in calculations of $\mathbf{J}^{(\mathrm{FC})}$ by Bartlett et al.

For chemical shifts, the calculations using the SCF wavefunctions, appear to give quite good results for CH_4 and other saturated ^{13}C sites, and even olefinic sites. The major problems that have been discovered for carbon are those environments (e.g. C≡O, –C≡N, and >C=O) for which electron correlation is extremely important. Electron correlation is important for ^{31}P calculations in molecules where a lone pair is on the phosphorus, even when only hydrogen atoms are attached to it. The SCF level has been found to be insufficient even for calculations using very large basis sets to reproduce the anisotropy of the ^{31}P shielding in the molecule PH_3.[13] In these cases, some level of post-Hartree–Fock theory is necessary in order to obtain meaningful results.

Shielding calculations including electron correlation effects at the level of MBPT(2) or MP2 may be carried out with a conventional common origin or may be used with any of the distributed origin approaches. An alternative approach to second-order electron correlation effects called *SOPPA* belongs to the family of propagator techniques, but is different from and not equivalent to MP2. Many quantum mechanical software packages provide MP2 level of wavefunctions. These are supposed to take care of the dynamic correlation effects and hence to improve results for closed shell systems where SCF already gives good results. When the degree of electron correlation contribution to the shielding is small, this level is usually sufficient to provide useful comparisons with experiment. When the difference between SCF and MP2 results is not small, then it may be necessary to go up to the MP4 level, with the corrections at MP2, MP3, and MP4 often alternating in sign. Despite its successes, the inherent problem with this approach is the slow convergence of the perturbation series for those systems

Encyclopedia of Analytical Chemistry, Online © 2006–2013 John Wiley & Sons, Ltd.

This article was published in the *Encyclopedia of Analytical Chemistry* in 2013 by John Wiley & Sons, Ltd.
DOI: 10.1002/9780470027318.a6109.pub2

(with strong correlation effects) where MBPT(2) or MP2 level is no longer adequate.

MCSCF wavefunctions may sometimes be necessary for calculations of shielding, when the electronic ground state cannot be adequately described by a single electronic configuration, i.e. a single Slater determinant. A multireference calculation can properly account for strong correlation effects if closed shell SCF is too poor as an initial approximation (e.g. in O_3, NSF, SO_2, N_2O_3 molecules). SCF methods completely fail for such systems. MCSCF wavefunctions generated using complete active spaces (CAS) and restricted active spaces (RAS) may be used with any of the distributed origin methods, spawning such methods as MCSCF/GIAO and MCIGLO (multiconfiguration individual gauge for localized orbitals). The MCIGLO formulation was presented formally by van Wullen and Kutzelnigg, and applied to appropriate cases such as carbenes and dinitrogen oxides. The dinitrogen oxides $(NO)_2$, $(NO)(NO_2)$, and $(NO_2)_2$ have strong correlation effects that affect the shielding tensors. The ^{15}N and ^{17}O shieldings have been measured in these molecules and the effects of correlation are particularly interesting in that they are of both signs. In the nitroso nitrogen, the electron correlation effect is to enhance deshielding, while in the nitro nitrogen the correlation effects are to increase shielding. Thus, in $(NO)(NO_2)$ the correlation effects are large and opposite in sign for the two types of N. Correlation contributions to the isotropic ^{15}N shielding range are -558 ppm in $(NO)_2$, $+61$ ppm in $(NO_2)_2$ and -63 and $+116$ ppm in $(NO)(NO_2)$.

If different electronic configurations dominate the wavefunction at different geometries, the calculation of the shielding surface also requires a computational method based on a multiconfiguration wavefunction. The MCSCF approaches are hampered by the same sort of problem because rather large active spaces are needed to obtain satisfactorily converged results. While static correlation effects on shielding arising from near degeneracies are efficiently treated by the MCSCF methods described above, MBPT (also known as MP perturbation theory) has been used to treat dynamical correlation effects.

One of the most successful approaches for the treatment of electron correlation is provided by CC theory. While ultimately based on a single determinant reference function, the exponential parameterization of the wavefunction ensures an efficient treatment of electron correlation. In particular, dynamic correlation effects are accounted for with nearly quantitative accuracy at a fraction of the cost needed to obtain similar precision with MCSCF approaches. Among the various schemes suggested in the literature, the CCSD approximation[14] in which single and double excitations are considered in the cluster operator, has proven especially useful in calculations of other molecular properties. CC approaches can be considered as infinite-order generalizations of the MBPT series. The implementation of GIAOs for the CCSD approach has been carried out by Gauss and Stanton,[15] and further augmented by a perturbative correction for connected triple excitations CCSD(T).[16] The principal advantage of the GIAO method is the ease with which high-level treatments of electron correlation may be handled by straightforward application of analytic derivative theory.

MCSCF/GIAO calculations for triple-bonded systems, in particular, HC≡N, HN≡C, MeC≡N, and MeN≡C, show that the electron correlation effects are large for the triple-bonded nuclei, especially the component perpendicular to the triple-bond axis, and largest for the terminal nucleus. For example, the electron correlation contribution to $\boldsymbol{\sigma}_\perp$ for ^{13}C shielding is $+47$ to $+54$ ppm in the $-N\equiv{}^{13}C$ nuclear sites and to $\boldsymbol{\sigma}_\perp$ for nitrogen shielding is $+87$ to $+79$ ppm in the $-C\equiv N$ sites.[17] These MCSCF/GIAO results do not compare as well with experiments as do the calculations by Gauss using the CCSD method.[15,16]

The ultimate level of theory would be FCI, but this is only possible for very small systems and is rarely used.[18]

The same general methods for multiple perturbations are used for calculating spin–spin couplings, with the difference that there are no gauge origin problems in spin–spin coupling calculations. All but the $\mathbf{J}^{(OD)} + \mathbf{J}^{(OP)}$ mechanisms mix triplet states with the unperturbed electronic singlet ground state. Thus, the unrestricted Hartree–Fock (UHF) method is sometimes used to generate the unperturbed electronic ground state, even for closed shell molecular systems such as CH_4. The extent to which electron correlation needs to be included depends on the system, just as in shielding calculations. The same molecules that are found to be pathological cases in shielding calculations also pose problems in spin–spin coupling calculations. The uncorrelated finite field SCF calculations, which are the same approximation as SCF and RPA calculations, in most cases give good results for $\boldsymbol{\sigma}$, while this is not often true for $\mathbf{J}$. The $\mathbf{J}^{(OD)}$ term in spin–spin coupling, similar to the diamagnetic part of $\boldsymbol{\sigma}$, is generally easy to calculate; good results can be obtained with low-level electronic correlation included and using moderately sized basis sets. The sum over all excited states in $\mathbf{J}^{(OP)}$ extends over singlet excited states as most of the common ground states that chemists are interested in are singlet states. However, in the $\mathbf{J}^{(SD)}$, $\mathbf{J}^{(FC)}$, and $\mathbf{J}^{(SDFC)}$ expressions, the excited states have different spin multiplicity from the ground state. Because there is a state of triplet symmetry either very close to or sometimes below the

Encyclopedia of Analytical Chemistry, Online © 2006–2013 John Wiley & Sons, Ltd.

This article was published in the *Encyclopedia of Analytical Chemistry* in 2013 by John Wiley & Sons, Ltd.
DOI: 10.1002/9780470027318.a6109.pub2

restricted Hartree–Fock singlet ground state for many molecules, these mechanisms for spin–spin coupling are very poorly described at the SCF-level of approximation. This problem affects spin–spin coupling calculations, but not calculations of $\boldsymbol{\sigma}$. Geertsen and Oddershede.[19] initiated a resurgence of interest in accurate *ab initio* calculations of coupling constants by using polarization propagator methods. The SOPPA has been found to yield reliable coupling constants in some instances. When higher accuracy is required, CCSD reference states (limited to single and double excitations) have been used within the polarization propagator method.[20,21] Midway between first (RPA) and second-order is HRPA (higher random phase approximation), which has been used to calculate one- and two-bond coupling constants, $^{1 \text{ or } 2}\mathbf{J}$(CC) in ring systems. MCSCF wavefunctions are appropriate in cases where the SCF calculations predict unrealistic coupling constants, such as in (pathological) molecules involving multiply bonded nitrogens. The method is MCLR (multiconfiguration linear response). MCSCF functions have been used for the hydrides of group IV (C, Si, Ge, Sn).[22] Bartlett et al. have used finite field methods to calculate the FC mechanism of spin–spin coupling using various levels including electron correlation, up to CCSD, and Stanton and Gauss[23] have used the analytic second- derivative approach.

The HD molecule is the smallest molecule for which the NMR indirect nuclear spin–spin coupling constant may be observed and at the same time a molecule for which *ab initio* quantum-chemical calculations may be performed at the most advanced levels of theory. For this molecule, the most complete electron correlation (FCI) nonrelativistic calculations including all four components of the tensor are possible.[24] For HD, a large zero-point vibrational correction of 1.89 Hz and a smaller but non-negligible temperature correction of 0.20 Hz, arriving at a theoretical isotropic value of 43.31(5) Hz at 300 K. Of this total value, the FC, SD, OP and OD terms are 98, 1, 2, and −1%. The experimental value is 43.26(6) Hz in the gas phase, extrapolated to zero density in He gas.

2.5 Density Functional Methods

One method of including electron correlation effects is through DFT. DFT methods are based on a theorem that states that for a scalar potential $V(\mathbf{r})$ the ground-state N-electron density uniquely determines the potential that gives rise to it. The total electronic energy is a unique functional of the density $\rho(\mathbf{r})$.[25] Although constructing an accurate approximation to the kinetic exchange correlation functional $G[\rho(\mathbf{r})]$ is a formidable task, it need only be done once because the form of G is independent of the form of $V(\mathbf{r})$. Approximations are required because the functional is not known exactly, but these approximations are getting better and better. Developments in exchange correlation functionals have made DFT methods viable alternatives to those of conventional quantum mechanical calculations. DFT combines the promise of accurate results (i.e. more accurate than Hartree–Fock-level quantum calculations) with cheaper computation (because it scales up to more electrons less steeply than conventional methods that include some electron correlation). Several approximate functionals of the electron density are in common use and are relatively successful in prediction of molecular structure, and are known to yield geometries and energies of at least MP2 quality.

The difficulties of calculating magnetic response properties using DFT arise in two major ways. The first is intrinsic to all DFT methods, because only approximate functionals are available and they are deficient in various ways. NMR parameters show up these deficiencies most glaringly because of their extreme sensitivity to the electron distribution in the immediate vicinity of the nucleus. The second difficulty is that in the presence of a vector potential (when magnetic fields or magnetic moments are present), the functionals of both the current density *and* the electron density are needed, thus a current density functional theory (CDFT) is the appropriate theory. A current-dependent DFT has been derived by Vignale et al.[26] On the other hand, more commonly, a generalization of the Kohn–Sham density functional theory (KSDFT) has been used to obtain magnetic responses using only the functional of the electron density; the current density part of the calculation is not included. This is by far the most commonly used calculation method. It remained to be shown by Grayce and Harris that when the magnetic field is produced by a constant applied field and a single nuclear magnetic dipole, the current density is a functional of the electron density. Furthermore, they showed that in the linear response regime, the current density functional depends on the *zero field electron density*. As a consequence, magnetic responses in the linear regime are solely functionals of the electron density in the absence of a magnetic field. Grayce and Harris[27,28] call this the *magnetic field density functional theory* (*BDFT*). The problem is that in all DFT approaches, only *approximate* functionals are available as of now, and the magnetic-response DFT approaches, whether CDFT, KSDFT, or BDFT, all suffer from this same difficulty.

There are several independent formulations of DFT of shielding. Initially, a large number of DFT calculations were carried out without including the effects of the current density, using a local density approximation (LDA) in an SOS method and an IGLO method of local origins for shielding tensor calculations. Lee, et al.[29]

Encyclopedia of Analytical Chemistry, Online © 2006–2013 John Wiley & Sons, Ltd.

This article was published in the *Encyclopedia of Analytical Chemistry* in 2013 by John Wiley & Sons, Ltd.
DOI: 10.1002/9780470027318.a6109.pub2

derived equations within the Kohn–Sham formulation of DFT for calculations of nuclear magnetic shielding tensors with GIAO basis functions using CDFT, including the use of a local exchange correlation functional that depends on both the electron density and the paramagnetic current density. To put the various DFT formalisms and calculations in context, they applied their working expressions to the systems HF, N_2, CO, F_2, and H_2O. By doing computations using conventional atomic basis functions versus GIAOs basis functions, using various local functionals of the density in popular use, such as the exchange functional of Becke with the correlation functional of Becke–Lee–Yang–Parr (BLYP) and others, with and without including the current-dependent functional proposed by Vignale et al. with or without the ad hoc correction of Malkin et al. Some very useful comparisons are provided by Lee et al.[29] They of course found what is already well known: using GIAOs leads to better results for σ than using conventional (gaugeless) atomic basis functions whether employing *ab initio* or DFT methods. They found that including the current-dependent functional proposed by Vignale et al. gives only small corrections. They also established that DFT and CDFT methods exhibit general difficulty in describing multiply bonded systems such as N_2 and CO. An important observation is that calculations using local functionals of the density give severely deficient eigenvalues. To overcome this, a more accurate functional must be developed. Since the Malkin correction is to modify the energy denominators, this has the effect of shifting the incorrect eigenvalues already noted above. Indeed, direct comparisons by Lee et al. using various functionals with and without the ad hoc Malkin correction lead to a significant improvement in the CO case. They also found that, unlike in the HF molecule, exchange terms are significant in the CO molecule and the current density terms are no longer negligibly small. The general conclusions are that the use of local density functionals is a major deficiency and overwhelms the small current density corrections.[29] The best results for CO in the Lee et al. formulation of CDFT/GIAO appear to come from the hybrid B3LYP (Becke, three-parameter, Lee–Yang–Parr) functional[30,31] combined with the Malkin correction.[32] Thus, in spite of what appears to be a lack of solid theoretical foundation, the ad hoc Malkin correction gives very promising results.

There are several other implementations of DFT in shielding calculations, all of which use only current-independent exchange correlation functionals, such as the GIAO-based DFT calculations introduced by Schreckenbach and Ziegler[33] and Pulay et al.[34] In practice, the calculations in the Ziegler DFT/GIAO implementation employ Slater-type orbitals as atomic basis functions (unlike most computations, which use Gaussian-type basis functions). Pulay et al. have developed a DFT/GIAO that uses the analytic derivative theory. Compared to the Hartree–Fock case, the only new quantity is the first-order exchange correlation term. In the Pulay implementation, these terms are evaluated by the same Becke numerical integration scheme they use for the exchange matrix elements themselves. Other implementations use DFT with the general CSGT (continuous set of gauge transformations) method of Keith and Bader[35] (wherein the current is determined through the definition of a CSGT, a separate gauge origin to calculate the current $\mathbf{J}^{(1)}(\boldsymbol{r})$ at each point $\boldsymbol{r}$ in real space).

How well does DFT predict absolute shielding? DFT accounts for correlation effects implicitly in the exchange correlation functionals used and thus might be expected to give superior results in comparison to SCF calculations for a given GIAO set of basis functions, in those molecules such as CO, N_2, NNO, and HCN where electron correlation effects on shielding are important. Absolute shieldings obtained using the gradient-corrected functionals are consistently better than SCF in these molecules, although the improvement is small in some cases. Using a basis set that is sufficient to predict accurate shifts using GIAO/MP2 theory, various DFT functionals consistently predict chemical shifts that are too deshielded compared with experiment. The absolute shielding results are too deshielded by 10–20 ppm for ^{13}C, by 6–40 ppm for ^{15}N, and by 30–40 ppm for ^{17}O in the selected molecules where the absolute shielding results are known. Anisotropies are even worse. The successful wide applicability of the DFT method for calculating $\boldsymbol{\sigma}$ lies in its applications to molecules with large numbers of electrons, where the accurate CCSD(T) calculations are not feasible and even MP2-level calculations are prohibitively expensive and impractical. CCSD(T) is the ''gold standard'' of computational quantum chemistry, against which other methodologies are typically compared. The test of any theoretical method for calculating $\boldsymbol{\sigma}$ is the comparison of the results with the benchmark CCSD(T) calculations of Gauss for a set of small molecules at the same fixed geometries. Benchmarking DFT calculations of $\boldsymbol{\sigma}$ by using accurate CC calculations have been carried out by Gauss et al.[36] The accuracy of the calculated coupled-cluster constants is established by a careful comparison with experimental data, taking into account zero-point vibrational corrections. Coupled-cluster basis-set convergence is analyzed and extrapolation techniques are employed to estimate basis-set-limit quantities, thereby establishing an accurate benchmark data set of all nuclei (H, Li, C, N, O, F, Al, P, and S, 72 nuclear sites in all) in 28 different molecules, many of which are ''pathological'' cases in terms of the importance of

Encyclopedia of Analytical Chemistry, Online © 2006–2013 John Wiley & Sons, Ltd.

This article was published in the *Encyclopedia of Analytical Chemistry* in 2013 by John Wiley & Sons, Ltd.
DOI: 10.1002/9780470027318.a6109.pub2

electron correlation and where relativistic effects are expected to be small. This level of theory, at which the calculated values are of a quality comparable to that of most measurements, was therefore selected as reference for the benchmarking of the various DFT functionals. The DFT approximations generally underestimate shielding constants, especially the LDA and general gradient approximation (GGA) functionals. The origin of this underestimation can be traced to a poor description of the paramagnetic contribution to the NMR shielding. This term has an inverse dependence on the occupied–virtual Kohn–Sham eigenvalue differences that tend to be too small. The paramagnetic contribution therefore becomes too negative and the overall shielding constant too low. Inclusion of some Hartree–Fock exchange leads hybrid DFT approaches [e.g. the popular B3LYP and PBE0 (Perdew–Burke–Ernzerhof hybrid) functionals] to outperform the LDA and GGA functionals, apart from the KT2 functional of Keal and Tozer. Even using the electronic density from the CCSD(T) wavefunctions does not lead to improved accuracy, therefore suggesting that the current density contributions of CDFT (mentioned above) are non-negligible and should be included in a consistent DFT treatment of NMR parameters.

The DFT method has severe limitations for the calculations of spin–spin coupling as well, which are connected to the inability of the presently available exchange correlation functionals (LDA and GGA) to produce the highly accurate spin densities required to describe properly the FC term for molecules containing atoms lying at the right of the periodic table and containing lone pairs. The $\mathbf{J}^{(\mathrm{OD})}$ term is the easiest to calculate, a straightforward numerical integration in the DFT method because this contribution depends only on the unperturbed ground-state density. The calculations of the $\mathbf{J}^{(\mathrm{OP})}$ and $\mathbf{J}^{(\mathrm{FC})}$ terms, just as in the *ab initio* calculations of $\mathbf{J}$, require the spin-unrestricted approach that is normally applied to open shell systems. The $\mathbf{J}^{(\mathrm{SD})}$ contribution is the most time-consuming and is usually neglected in DFT calculations of $\mathbf{J}$ because it is usually smaller than the error in the $\mathbf{J}^{(\mathrm{FC})}$ calculation by this method. A fully analytical implementation of $\mathbf{J}$ including all four terms for use with LDA, GGA, and hybrid functionals has been provided by Helgaker et al.[37,38] Improved results will require a better exchange correlation functional to describe the spin polarization more precisely. A parameterized functional trained to reproduce a set of gas-phase, isotropic, hyperfine coupling constants in nonsinglet radicals might be a good start.

Despite its limitations, DFT method is widely used in calculations of NMR parameters; the advantage of DFT is that it can be routinely applied to very large molecules, providing results of comparable quality as for small molecules. This is the reason that DFT has been the workhorse of computational chemistry for several decades; the major drawback is that systematic routes to improve the exchange correlation functionals have not been found.

2.6 Relativistic Calculations

Although all electrons are affected by relativity, the effect is most pronounced for those molecular properties whose quantum mechanical operators involve steep inverse powers of radial distance of the electron, such as r^{-3} or even a delta function at the nucleus. As seen in Equations (9)–(14), the nuclear magnetic shielding and the indirect nuclear spin–spin coupling have these forms of the operators and should be more strongly affected by relativity than properties that depend predominantly on valence electrons such as the electric dipole polarizability. A relativistic treatment is therefore often needed for NMR parameters, spin–spin coupling – in particular, for those molecules that involve heavy nuclei. It is well known that relativistic effects are very important in the study of heavy elements.

Instead of the Schrödinger equation, one has to solve a many-electron generalization of the four-component Dirac equation; these are the four-component methods based on the Dirac–Coulomb Hamiltonian. The magnetic perturbation operators are linear in the vector potentials of $\vec{A}_0$ and $\vec{A}_M$ in the Dirac Hamiltonian, while they are quadratic in the Schrödinger Hamiltonian. Therefore, there is no resemblance between the relativistic and nonrelativistic expressions for the diamagnetic shielding. Fully relativistic calculations are very time-consuming even at the Dirac–Hartree–Fock level. There is also the relativistic polarization propagator approach for calculations of J and shielding by Oddershede et al.[39] Including electron correlation at the same level as is available in nonrelativistic theory is even more demanding. Relativistic CCSD and configuration interaction singles and doubles methods have been developed by Nakatsuji et al.[40] but is practical only for small molecules. To include electron correlation efficiently within a relativistic four-component treatment, a DFT approach for the calculation of nuclear shieldings and J has been developed by Malkin et al.[41] and Pecul et al.[42] There are also two-component methods, ''exact''[43] and approximate. Of the former, there are several approaches;[44] of the latter, some are based on the regular approximation [e.g. the popular ZORA (zeroth-order regular approximation) method] or on the Douglas–Kroll–Hess Hamiltonian. Finally, there are approximate methods that employ perturbative corrections on top of a nonrelativistic treatment.

Encyclopedia of Analytical Chemistry, Online © 2006–2013 John Wiley & Sons, Ltd.

This article was published in the *Encyclopedia of Analytical Chemistry* in 2013 by John Wiley & Sons, Ltd.
DOI: 10.1002/9780470027318.a6109.pub2

The relativistic effects on shielding may be considered in three parts. One is the direct effect of the relativistic contraction of s and p inner shells and the relativistic SCF expansion of d and f shells on the diamagnetic contribution. The contraction of the s and p shells leads to larger values of $\langle r_{kN}{}^{-3}\rangle$ and $\langle r_{kN}{}^{-1}\rangle$. The essentially constant relativistic effect on the diamagnetic contribution from the core electrons can be a large correction but it hardly changes as the atom is compared from one molecule to the next. This is of little concern while taking differences, namely, the chemical shifts. Another relativistic effect is the indirect effect of this s and p contraction and d and f expansion within the Hartree–Fock scheme, an effect that varies from one molecule to the next. Both of these relativistic effects are scalar or ''spin-free'' in nature. A third effect is that of introducing the electron spin–electron orbital angular momentum coupling, the so-called spin–orbit terms. To calculate the additional contributions to the nuclear magnetic shielding associated with spin–orbit interactions, the latter has been approached approximately by a nonrelativistic treatment with the spin–orbit operator added on as a perturbation. These corrections can be large for nuclei whose immediate neighbors are atoms that have large values of spin–orbit coupling constants, e.g. the heavier halogens. Both the spin-free relativistic term and the spin–orbit terms can be important and they can couple with each other, as they do in ^{199}Hg shielding in mercury halides. One way of approximately including relativistic effects in nonrelativistic calculations is to use relativistic effective core potentials. The so-called normal halogen dependence of chemical shifts (increasing shielding on substitution of neighboring atoms by Cl, Br, I, in that order, sometimes called the HALA effect of heavy atom on light atom), which had previously been attributed to relativistic effects,[45] has been accounted for entirely by the spin–orbit contributions centered on the halogen atoms in approximate calculations of shielding of ^{1}H, ^{13}C, ^{29}Si, ^{71}Ga, and ^{115}In nuclei in the respective halides by Nakatsuji et al.[46] These approximate calculations have established the importance of the spin–orbit terms for shielding of nuclei having Cl, Br, and I neighbors. However, calculations of heavy atom shielding are not yet on a sound footing at the level of relativistic theory used here. Furthermore, the number of electrons involved is large and basis sets used are far from saturated so that it is not yet possible to have good nonrelativistic baseline values against which it may be possible to judge quantitatively that the relativistic approximations used are bridging the gap between nonrelativistic calculations and experiment. The second problem, which is just as important, is the lack of experimental absolute shielding data in the gas phase for such heavy nuclei. This leads to comparisons of theoretical values with solution data where solvent effects may even bring some doubt as to the actual chemical species being observed. The problem is particularly severe with the calculations involving bare anions of In, for example, rather than neutral species.

The electron-coupled nuclear spin–nuclear spin coupling **J** is itself a purely relativistic phenomenon. However, starting from a relativistic Hamiltonian such as the Dirac–Coulomb–Breit Hamiltonian, and neglecting the small components of the four component functions, the expressions for the spin–spin coupling tensor in the nonrelativistic limit (Equations 10–14) had been derived[5] and used in nonrelativistic calculations of **J**.

Aucar and Oddershede[47] formulated a fully relativistic *ab initio* theory of the spin–spin coupling in its most general form within the polarization propagator approach. They neglected the Breit interaction to derive the formulas that look very much like the nonrelativistic expression for spin–spin coupling in the propagator approach, except that the elements involve integrals of the full four component wavefunctions. The large component of the relativistic wavefunction is the nonrelativistic wavefunction. One relativistic expression replaces the nonrelativistic $\mathbf{J}^{(OP)}$, $\mathbf{J}^{(SD)}$, and $\mathbf{J}^{(FC)}$ terms. The theory leads to the nonrelativistic expressions in Equations (10)–(14) in the limit that the speed of light goes to infinity. Two-component relativistic methods for *J* have been implemented at the Hartree–Fock and DFT levels of theory.[48] As an early pioneer in the relativistic treatment of **J**, Pyykkö[11] derived a relativistic analog to Ramsey's theory, using a relativistic nuclear Zeeman hyperfine Hamiltonian as a perturbation; implementation has been limited to one-bond couplings.[49] The study of relativistic corrections to spin–spin coupling is not as advanced as for shielding; systematic improvement is hampered by some contributions diverging when basis sets are extended. There are as yet few four-component fully relativistic calculations of **J** for a large set of molecules. In addition, many reported calculations include relativistic contributions piece-meal, as scalar effects only or spin–orbit effects only, whereas it would be desirable to treat all contributions at the same level of theory. A further problem in **J** coupling calculations is that there is no consensus on the appropriate nuclear model to use. Four-component approaches use finite Gaussian-type charge distributions; two-component approaches use point charge models. Little is known about how the nuclear model affects the quality of relativistic **J**. Nevertheless, it is well established that when at least one of the coupled nuclei is a heavy nucleus, or when a heavy nucleus is on the coupling path, relativistic effects cannot be neglected. A popular method for heavy nuclei is

Encyclopedia of Analytical Chemistry, Online © 2006–2013 John Wiley & Sons, Ltd.

This article was published in the *Encyclopedia of Analytical Chemistry* in 2013 by John Wiley & Sons, Ltd.
DOI: 10.1002/9780470027318.a6109.pub2

ZORA-DFT, which is an approximate two-component approach.

Relativistic calculations in applications to EFGs have received less attention; for EFGs, there are scalar and spin–orbit contributions also. Four-component CC calculations have been carried out for Hg in HgX_2 (with X = Me, Cl, Br, I).[50] Two-component formalisms using exact methods of decoupling positive and negative energy solutions have been applied to EFGs, but additional corrections need to be made to correct for so-called picture change effects, which are sometimes large for EFGs.[44]

A perspective article on relativistic effects for chemists by Autschbach[51] is an accessible and generally useful guide, with particular examples for NMR shielding and **J** coupling. The comprehensive review *Relativistic Computations of NMR Parameters from First Principles* by Autschbach is likewise accessible with many examples.[52] A unified approach to four-component relativistic treatment of magnetic properties and a logical systematic classification of existing methods of calculations of NMR parameters within relativistic quantum chemistry has been presented by Kutzelnigg and Liu.[53] In this rigorous treatise, they critically explore various approaches to four-component calculations in a general context and also the commonly used approximate methods such as the Douglas–Kroll–Hess approximation and the ZORA in context. This places the various methods from a confusing melange in the literature onto a common consistent framework, which makes sense for finding relationships between methods and making comparisons among them.

2.7 Calculations in Periodic Systems

So far we have considered theoretical approaches for calculations of NMR parameters in a single molecule or a cluster of small molecules in a vacuum, where the system involves a finite number of electrons and nuclei. In such calculations, a systematic improvement of the accuracy of the results is possible by using a hierarchy of computational approaches all the way up to the ultimate ''platinum standard'': FCI. On the other hand, periodic systems, such as crystalline solids, have translational symmetry that can be exploited in calculations, while doing calculations on a system that is closer to the actual solid materials on which solid-state NMR observations are made.

The operators responsible for shielding and indirect spin–spin coupling are very short-ranged, involving at worst r^{-3} for the electronic distance from the nucleus. Why then do we need a solid-state approach for the calculation of NMR parameters? The quantities the operators act on – wavefunctions and electronic charge density – are influenced by the long-range atomic configurations and electrostatics of the material. This is true for all NMR parameters: **σ**, **J**, EFG. The particular way in which a protein is folded in its native state, the particular configuration of atoms that are remote from the observed nucleus in terms of bond connectivity, influences the dihedral angles in the immediate vicinity of the observed nucleus, thus affording a measurable discrimination between the alpha carbons of the many different alanines in the same protein and in different proteins. The sensitivity of the NMR parameters to these slight differences in chemical environment are an advantage for NMR as an analytical method and at the same time pose a challenge for accurate calculations of these parameters. Slight differences in bond distances and angles give rise to measurable changes in the NMR parameters for nuclei in solids, particularly the nuclear shielding, thus permitting distinction between different polymorphs of the same chemical compound in molecular solids, or between different crystal morphologies in covalent solids. **J** coupling across hydrogen bonds engendered by proximity between distinct molecules in the solid state, for example, **J** coupling across an intermolecular hydrogen bond, has been observed. These can only be calculated using a solid-state approach.[54]

How should one deal with these translationally periodic networks? Density functional approaches to electronic structure of solid materials had been available for some time, but the first approach for calculating NMR chemical shifts in solids was developed by Mauri[55]; this method could be applied to periodic systems such as crystals, surfaces, or polymers and, with a supercell technique, to nonperiodic systems such as amorphous materials, liquids, or solids with defects, or isolated molecules. This method and its improved versions are in wide use. Subsequently, several alternative DFT methods under periodic boundary conditions have been proposed and applied to the same benchmark solids as Mauri for direct comparisons. See the similarities and differences between these emerging methods in a review, Ref. 56

Mauri overcame the inherent difficulty that the position operator that explicitly enters the perturbed Hamiltonian for NMR is not well defined for periodic systems, and the task of computing the induced current is complicated by the fact that the magnetic field breaks translational symmetry. Improvements to the original approach have been incorporated by Mauri et al.[57] in the version called the *GIPAW* (*gauge-including projected augmented wave*) method. The method uses pseudopotentials. In the pseudopotential approach, only the valence electrons are explicitly considered, the effects of the core electrons being integrated within a new ionic potential. The method reconstructs all-electron density close to atomic nuclei, correctly accounting for

Encyclopedia of Analytical Chemistry, Online © 2006–2013 John Wiley & Sons, Ltd.

This article was published in the *Encyclopedia of Analytical Chemistry* in 2013 by John Wiley & Sons, Ltd.
DOI: 10.1002/9780470027318.a6109.pub2

electrons in this region. Fourth-row elements, transition, and rare-earth metals require very large numbers of plane waves to accurately describe the valence wave functions. For these, more efficient pseudopotentials have been designed, ''ultrasoft'' pseudopotentials, which are as soft as possible in the core region and require a minimum number of plane waves for full convergence and GIPAW has been reformulated to make use of these.[58] Mauri et al.[59] have also developed a calculation of relativistic effects on chemical shifts in solids using the ZORA, and a theory of *J* in solids.[60] To compute the EFG tensor in a periodic system is less demanding than calculating either the shielding or indirect coupling tensors, as it requires only knowledge of the ground-state charge density, ground-state wavefunctions and the position of the nuclei in the unit cell. For quadrupolar nuclei, both the EFG and chemical shift tensors are required in the interpretation of the spectra, thus, executing both calculations within the same computational framework in GIPAW is convenient. With the availability of reliable pseudopotentials, GIPAW method has been widely used in the solid-state NMR community as a routine tool for structural assignment/interpretation and understanding of nuclear site electronic structure, particularly in cases with several nuclear sites. An accessible review of the theory for all three NMR parameters is given by Yates and Pickard,[61] and a review of calculations of *J* in solids by Yates.[62] GIPAW and the other methods for periodic systems permit calculations of NMR parameters ''in situ'' for covalent solids, ionic solids, strongly hydrogen-bonded solids, proton-conducting molecular crystals, and polymorphs where slight differences in NMR parameters and other properties arise from small differences in crystal-packing forces for the same chemical structural formula.

3 CALCULATIONS OF NUCLEAR MAGNETIC RESONANCE CHEMICAL SHIFTS

3.1 Comparison of Various Computational Methods Using the Same Set of Test Molecules

Which method would be best to use for calculating NMR chemical shifts? The answer depends on the question being asked. Is the chemical shift to be used to discriminate between two or more proposed chemical structures? Is the goal to verify a particular structure? Is it to determine whether the molecule is fluxional, whether it forms a complex, on the basis of the NMR chemical shifts? Is it to assign the multitude of peaks observed in a crystalline sample? Sometimes, we just want to understand what it is about the electronic structure that gives rise to an observed chemical shift or its temperature dependence. Depending on the accuracy that is required to answer the question being asked, a particular method and level of calculation and a particular size of basis set may be sufficient. It is not always necessary to use the most accurate method and the largest basis set. But first, we compare methods across the board, using several benchmark molecules, in order to see the level of accuracy that may be expected.

We present some comparisons of absolute isotropic shieldings calculated using GIAOs in Tables 1 and 2. The calculations are for a fixed geometry, and therefore should be compared with the value for the equilibrium geometry of the molecule, σ_e, whereas the room temperature average value in the limit of zero density, $\sigma_0(300\,\mathrm{K})$, is for a rotating vibrating molecule. Electron correlation effects on the individual components of the tensor differ and so are partly washed out in the isotropic average value (which is one-third the sum of the principal components of the tensor). Nevertheless, these comparisons are revealing. Here, we included the various levels of many body perturbation expansion MBPT(2), MBPT(3), MBPT(4) used by Gauss,[64] the CCSD approximation augmented by a correction for triple excitations (CCSD(T)) by Gauss et al.,[36] an FCI calculation for BH molecule by Gauss and Ruud,[18] and the MCSCF results using GIAOs from Ruud et al.[17,65] We also include the results from DFT using the simplest LDA functional and the KT2 functional of Keal and Tozer, and earlier calculations in the generalized gradient approximation using the exchange functional of Becke with the correlation functional of Lee–Yang–Parr DFT/BLYP from calculations using the different implementations of Pulay et al.[34] and Schreckenbach and Ziegler[33]

Examination of Tables 1 and 2 permit the following conclusions. For the hydrides HF, H_2O, NH_3, and CH_4, electron correlation effects described by triple excitations are small, amounting to <1 ppm for the nonhydrogen nuclei. The effects for proton shieldings are not shown in the tables, but they are even smaller, of the order of 0.1 ppm. MBPT(4), CCSD, and MCSCF all provide an adequate treatment of electron correlation effects for these simple systems. Furthermore, the agreement with experiment is very good. It has been found in systematic studies of a large number of ^{13}C chemical shifts that MBPT(2)-level results are much closer to experiment than CCSD results.[66] It appears that MBPT(2) benefits from a fortuitous but consistent error cancellation, while CCSD (which is theoretically more complete and is in principle a more reliable approach) does not. Triplet excitation effects are considerably more important for the multiply bonded systems CO, N_2, and HCN. The magnitude of the triplet excitation corrections (2–6 ppm)

Encyclopedia of Analytical Chemistry, Online © 2006–2013 John Wiley & Sons, Ltd.

This article was published in the *Encyclopedia of Analytical Chemistry* in 2013 by John Wiley & Sons, Ltd.
DOI: 10.1002/9780470027318.a6109.pub2

Table 1 Comparison between absolute shielding calculations, all using GIAOs and experiment[a]

Method	^{13}C in CH_4	^{13}C in CO	^{13}C in HCN	^{15}N in NH_3	^{15}N in N_2	^{15}N in HCN
DFT/LDA[b]	193.1	−20.3	65.3	266.3	−91.4	−56.7
DFT/KT2[b]	195.2	7.4	86.0	264.5	−59.7	−19.4
DFT/BLYP[c]	187.8	−12.2	71.7	259.4	−80.6	−43.5
DFT/BLYP[d]	191.2	−9.3	91.5	262.0	−72.9	8.4
SCF[e]	194.8	−25.5	70.9	262.3	−112.4	−50.7
MBPT(2)[e]	201.0	10.6	87.6	276.5	−41.6	−0.3
MBPT(3)[e]	198.8	−4.2	80.0	270.1	−72.2	−26.2
MBPT(4)[e]	198.6	4.1	84.3	269.9	−60.1	−14.9
MCSCF	198.2[f]	8.22[f]	86.76[g]	—	−52.2[f]	2.63[g]
CCSD[b]	198.81	−0.95	83.4	268.8	−64.7	−16.9
CCSD(T)[b]	199.2	4.0	85.7	270.8	−58.8	−12.7
Expt. σ_0[h]	195.0 ± 1	0.9 ± 0.9	82.1 ± 0.9	264.5 ± 0.2	-61.6 ± 0.2	-20.4 ± 0.2
Emp. σ_e[i]	198.7	3.3	84.4	273.3	−57.3	−10.2

[a] σ_e values are the ones that should be compared with the calculations. All shielding values are in ppm.
[b] Gauss et al.[36] (KT2 is a functional designed by Keal and Tozer.[63])
[c] Pulay et al.[34]
[d] Ziegler et al.[33]
[e] Gauss[64]
[f] Ruud et al.[65]
[g] Barszczewicz et al.[17]
[h] These are absolute shielding values σ_0, which are isotropic averages in the gas at the zero-pressure limit. They correspond to the thermal average for an isolated molecule.
[i] The estimates of the vibrational corrections have been subtracted from σ_0 to obtain the empirical value σ_e (the value for a rigid isolated molecule at its equilibrium molecular geometry) with which calculations are to be compared. See Gauss et al.[36] for the references for experimental data and vibrational corrections.

Table 2 Comparison between absolute shielding calculations, all using GIAOs and experiment[a]

Method	^{17}O in H_2O	^{17}O in CO	^{19}F in HF	^{19}F in F_2	^{1}H in BH	^{11}B in BH
DFT/LDA[b]	334.8	−87.5	416.2	−284.2	—	—
DFT/KT2[b]	329.6	−57.1	412.4	−211.0	—	—
DFT/BLYP[c]	326.4	−73.6	410.9	−277.1	—	—
DFT/BLYP[d]	331.5	−68.4	412.5	−282.7	—	—
SCF[e]	328.1	−87.7	413.6	−167.9	24.21	−261.25
MBPT(2)[e]	346.1	−46.5	424.2	−170.0	24.12	−220.67
MBPT(3)[e]	336.7	−68.3	417.8	−176.9	24.14	−201.92
MBPT(4)[e]	337.5	−52.0	418.7	−174.0	24.22	−184.18
MCSCF[f]	335.3	−38.92	419.6	−136.6	—	−174.83[g]
CCSD[b]	337.0	−56.8	419.7	−175.2	24.74	−166.64
CCSD(T)[b]	338.0	−53.6	420.2	−182.1	24.62	−170.46
FCI[g]	—	—	—	—	24.60	−170.08
Expt. σ_0[h]	323.6 ± 0.3	-62.7 ± 0.3	409.6 ± 1	-232.8 ± 1	—	—
Emp. σ_e[i]	337.83	−57.0	421.7	−192.8	—	—

[a] σ_e values are the ones that should be compared with the calculations. All shielding values are in ppm.
[b] Gauss et al.[36] (KT2 is a functional designed by Keal and Tozer.[63])
[c] Pulay et al.[34]
[d] Schreckenbach and Ziegler [33]
[e] Gauss[64]
[f] Ruud et al.[65]
[g] Gauss and Ruud[18]
[h] These are absolute shielding values σ_0, which are isotropic averages in the gas at the zero-pressure limit. They correspond to the thermal average for an isolated molecule.
[i] The estimates of the vibrational corrections have been subtracted from σ_0 to obtain the empirical value σ_e (the value for a rigid isolated molecule at its equilibrium molecular geometry) with which calculations are to be compared. See Gauss et al.[36] for the references for experimental data and vibrational corrections.

Encyclopedia of Analytical Chemistry, Online © 2006–2013 John Wiley & Sons, Ltd.

This article was published in the *Encyclopedia of Analytical Chemistry* in 2013 by John Wiley & Sons, Ltd.
DOI: 10.1002/9780470027318.a6109.pub2

Table 3 Calculated ^{13}C chemical shifts (in ppm) relative to $^{13}CH_4$, and experimental values in the gas phase

A	σ (CH_4) – σ(A), calculated		Expt.[b]
	SCF[a]	MBPT(2)[a]	
CH_3CH_3	11.7	13.5	14.2
$H_2C{=}CH_2$	135.8	130.3	130.6
$HC{\equiv}CH$	81.8	78.2	77.9
CH_3F	71.6	79.7	78.3
CH_3OH	52.0	59.3	58.5
CH_3NH_2	31.9	36.6	36.8
CH_3CHO	33.5	38.7	37.9
$(CH_3)_2CO$	32.2	37.0	37.1
CH_3CN	4.8	7.9	7.4
CO	224.9	190.4	194.1
CO_2	147.9	138.0	136.3
H_2CO	205.0	194.8	—
CH_3CHO	211.3	200.3	201.8
$(CH_3)_2CO$	218.8	207.3	208.2
HCN	127.5	114.2	113.0
CH_3CN	135.1	125.4	121.3
$CH_2{=}C{=}CH_2$	240.0	227.5	224.4
$CH_2{=}C{=}CH_2$	81.7	80.6	79.9
CF_4	116.4	137.1	130.6
C_6H_6	140.6	137.5	137.9

[a]Gauss[67]
[b]Jameson and Jameson.[68]

for these systems leads to calculated results that are closer to experiment. For the F_2 molecule, inclusion of triple-excitation corrections leads to a change of about 15 ppm and brings the calculated value closer to experiment. Results for F_2 at lower levels of calculation do not provide satisfactory agreement with experiment. Except for the F_2 molecule, GIAO/MCSCF calculations using very large active spaces (only those are shown in Tables 1 and 2) provide results comparable to CCSD. It has been found, and is obvious in Tables 1 and 2, that the DFT method consistently overestimates the paramagnetic term leading to too much deshielding for these benchmark molecules. The SCF value is good enough for CH_4, NH_3, and HF molecules to agree reasonably with the thermal average value (as the neglect of electron correlation effects in these and most molecules is compensated for by the neglect of rovibrational averaging), whereas the SCF level of theory is clearly inadequate for the multiply bonded CO, HCN, and N_2, and also for H_2O and F_2.

The benchmark test molecules shown in Tables 1 and 2, except for CH_4, are specifically chosen as examples that present problems of electron correlation, especially in ^{15}N, ^{17}O, and ^{19}F shielding. Observe in Tables 1 and 2 the slow convergence in some molecules, faster in others, of the series SCF, MBPT(2), MBPT(3), and MBPT(4). Observe also the consistent improvement over SCF afforded by the approximate exchange correlation functionals used in DFT calculations, especially for CO, N_2, HCN. Observe also how close CCSD(T) results come to the FCI (in BH molecule). More typical of the applications of calculated NMR chemical shifts to analysis of mixtures are calculations of ^{13}C chemical shifts. Table 3 demonstrates the importance of electron correlation to ^{13}C chemical shifts in comparison with chemical shifts in the gas phase at the low density limit. It can be seen that the second-order electron correlation generally brings the calculations close enough to experiment to be useful for analysis.

3.2 Comparison of Carbon Chemical Shift Tensor Components with Calculations

A more stringent test of the calculations has to do with reproducing the elements of the shielding tensor, not just the isotropic average that is obtained in solution or the average in an MAS experiment in the solid state. In a single-crystal study of a sugar, for example, there are a large number of peaks that have to be assigned in order to verify the structure. Complete assignment of ^{13}C shielding tensors in the entire molecule from single-crystal studies has been developed to the highest level by Grant et al.[69] The multiple-axis sample reorientation mechanism developed in this group permits the study of crystals containing 50–100 magnetically different nuclei per unit cell. In a polycrystalline solid with a very large number of distinct ^{13}C chemical sites, it is possible, using multidimensional NMR techniques, to obtain the individual shielding tensor elements for each isotropic peak in the MAS NMR spectrum. To assign all these, *ab initio* calculations of shielding tensor elements are indispensable.

How well do calculations predict the tensor elements? It is important to be able to do these calculations in a relatively routine manner (one cannot use CCSD level of calculations) so that fitting to the observed spectra can be done expeditiously. Otherwise, theoretical calculations would not be practically useful for analysis. The group of D. M. Grant has carried out the largest number of such analyses.[69] Single-crystal NMR experiments produce a complete description of the shielding tensor with six independent components specifying the tensor in a fixed crystallographic coordinate system (the so-called icosahedral tensor representation). Figure 1 shows the degree of success of SCF-level calculations using a modest-size basis set.[70] The high level of agreement between calculated and experimental tensors for ^{13}C is such that only the structural parameters (bond distances and angles) limit the level of agreement. This means that *ab initio* calculations and measurements together can be used to address certain fine details of solid-state structure, surpassing the accuracy of X-ray data.[71] This is possible

Encyclopedia of Analytical Chemistry, Online © 2006–2013 John Wiley & Sons, Ltd.

This article was published in the *Encyclopedia of Analytical Chemistry* in 2013 by John Wiley & Sons, Ltd.
DOI: 10.1002/9780470027318.a6109.pub2

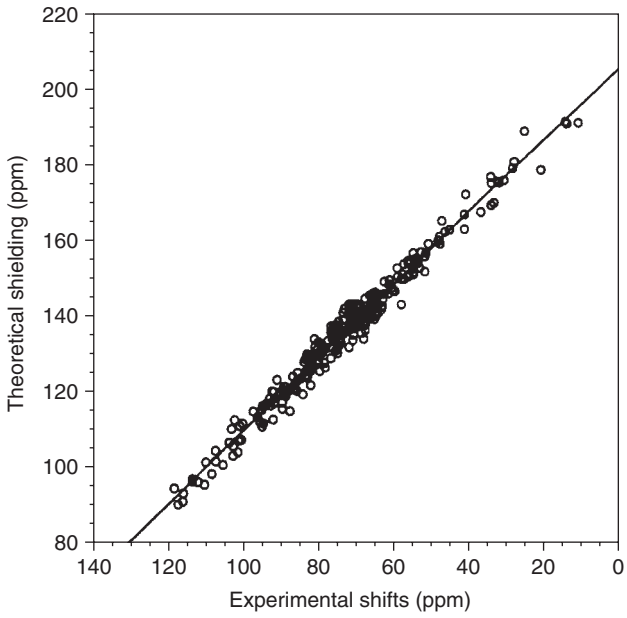

Figure 1 Comparison of computed full ^{13}C shielding tensors versus experimental values of icosahedral shift from TMS obtained from single-crystal measurements. Both are expressed in the icosahedral representation that includes the principal axis system orientation. (Reproduced with permission from Ref. 70. Copyright 1996, American Chemical Society.)

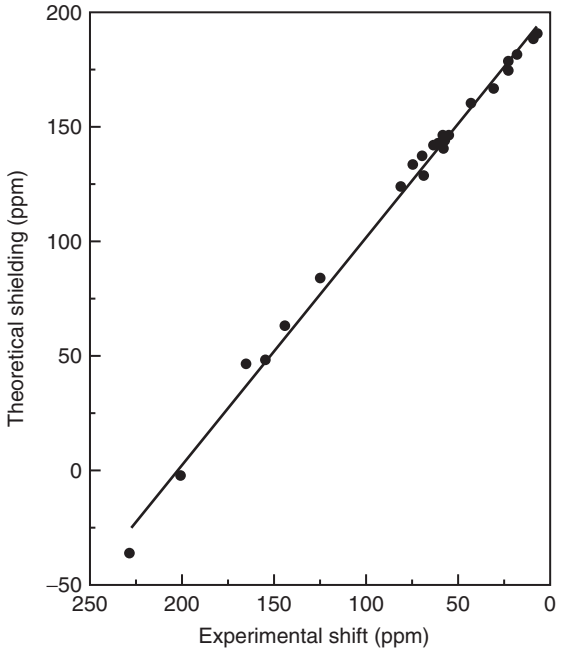

Figure 2 Comparison of computed full ^{13}C shielding tensors versus experimental values obtained from single-crystal measurements for threonine. Both are expressed in the icosahedral representation that includes the principal axis system orientation. (Reproduced with permission from Ref. 72. Copyright 1994, American Chemical Society.)

because the shielding tensor is exquisitely sensitive to bond distances.

It is quite important to be able to predict theoretically the individual tensor components of the building blocks of proteins, in order to establish that it is possible to use NMR chemical shifts in the determination of protein structure. In Figure 2 is the demonstration of the degree of success of SCF-level calculations using a modest basis set for the tensor elements of ^{13}C in a single crystal of threonine.[72]

3.3 Other First-Row Nuclei

Shielding calculations for N, O, and F in most molecules require a theoretical treatment including electron correlation. Gauss et al. established the benchmarks of shielding for these nuclei in sets of single molecules with large atomic basis sets, using CCSD theory and CCSD(T) theory, and these have been tested against absolute shieldings for these nuclei by including vibrational and temperature averaging corrections. Their benchmarks for the shielding of N,[73] O,[74] and F[75] nuclei have been used for testing the performance of less accurate but more practical medium-size bases for MP2 or various functionals for DFT calculations, prior to applications to bigger molecules of interest. A comprehensive study of 28 small molecules and 72 nuclear sites (all but 6 being first-row nuclei), using large basis sets and up to CCSD(T) level of theory, tested against absolute shieldings for these nuclei by including vibrational and temperature averaging corrections, provides a means of comparing various exchange correlation functionals in DFT calculations,[36] as already mentioned in Section 2.5. *Ab initio* calculations for ^{17}O are of sufficiently high quality to indicate that the absolute shielding for ^{17}O in CO (used to define the experimental absolute shielding scale) is very likely at the lower edge of the reported error bars. A systematic study of B, N, O, and F shielding using the IGLO method of distributed origins provided a measure of the initial successes of theoretical calculations for these nuclei in systems of known structure.[7] ^{11}B NMR chemical shift calculations have been routinely used for the analyses of new boron compounds, which are particularly useful when more than one structure can fit the electron diffraction data. DFT and *ab initio* methods with relativistic corrections have been used for ^{17}O shielding calculations in carbonyl complexes of transition metals (Ti, Zr, Hf, Fe, Rh, Cr, Mo, and W) by Kaupp et al. and also by Ziegler et al. In ^{17}O experiments used to validate the calculations, the anisotropy of the tensor $(\sigma_{||} - \sigma_{\perp})$ gives a good measure of the predictive success of ^{17}O calculations.[76,77]

Encyclopedia of Analytical Chemistry, Online © 2006–2013 John Wiley & Sons, Ltd.

This article was published in the *Encyclopedia of Analytical Chemistry* in 2013 by John Wiley & Sons, Ltd.
DOI: 10.1002/9780470027318.a6109.pub2

3.4 Second-Row Nuclei

Systematic studies of the shielding of nuclei ^{29}Si, ^{31}P, ^{33}S, and ^{35}Cl using IGLO distributed origins in a wide variety of molecules have been compared against chemical shifts, leading to reasonably good straight lines.[7] GIAO calculations including second-order MP2-level electron correlation for ^{31}P has been used to estimate the infinite-order results, and these agree very well with the absolute shieldings that are known for molecules ranging from PN to P_4 a range of about 900 ppm.[78] A similar systematic study was carried out for ^{33}S shielding in a wide variety of sulfur compounds spanning a wide range of chemical shifts, of 1000 ppm.[79] DFT calculations of ^{35}Cl shielding in XCl_4 (where X = C, Si, Ge, Sn, and Ti) gave good agreement with experimental chemical shifts observed in solution[80]; however, the calculations were not validated against any of the available absolute shieldings, such as in CIF ($\sigma = -516 \pm 23$ ppm) or HCl ($\sigma = 946.3 \pm 0.9$ ppm). Since many Cl NMR spectra are obtained in the solid state, subsequent calculations have been carried out using GIPAW.[81]

3.5 Heavy Nuclei

Heavy nuclei present some general problems for calculations of NMR shielding. First, the larger number of electrons requires larger numbers of basis functions and including electron correlation becomes very expensive. Second, relativistic effects could be very important as these tend to increase by powers of the atomic number. Third, in some cases there are few if any gas-phase data that can be used to test the absolute shieldings from the calculations; in many cases, only solution-phase experimental data is available for comparison with calculations (e.g. ^{69}Ga, ^{115}In, ^{75}As, ^{121}Sb, ^{129}Xe). For the heavier nuclei, the nonrelativistic identity that relates the spin–rotation tensor, measured in the isolated molecule via microwave spectroscopy, to the paramagnetic part of the nuclear shielding no longer holds. The intuitive zero paramagnetic shielding along the axis of a linear molecule that arises from nonrelativistic theory no longer holds, which means that the parallel component of the $[\boldsymbol{\sigma}^{Xe}(FXeF) - \boldsymbol{\sigma}^{Xe}(atom)]$ chemical shift tensor is not zero or nearly zero. The observation by Wasylishen et al. of a nonzero parallel component for Xe chemical shift in XeF_2 relative to the Xe atom establishes experimentally that the relativistic effects on Xe chemical shifts cannot be neglected. The relativistic contributions to the Xe atom shielding are easily understood to be large, but this experimental finding means that the relativistic contributions do not subtract out in taking chemical shifts because they vary substantially from one molecular system to the next.

^{77}Se is an exception to the third difficulty; there are gas-phase data for Se compounds and these can be used to explore the range of problems associated with heavy nuclei in general. Correlation effects must be included for a quantitative description of ^{77}Se chemical shifts in those same bonding situations where ^{17}O shielding has been found to require correction for correlation effects. The additional complication of the large number of electrons therefore makes the ^{77}Se calculations more challenging. The results of *ab initio* calculations are very good. At the SCF level, for example, various calculations for the isotropic shielding of H_2Se lead to 2167.6, 2170, and 2171 ppm, which are very close to each other and reasonably close to the value calculated at the CCSD level (2213 ppm) and the experimental value: 2101 ± 64 ppm on the absolute shielding scale[82] (without the relativistic corrections for the diamagnetic shielding of the free atom). The electron correlation effects are only 2% of the total shielding in H_2Se and O=C=Se; they are 7% of the total shielding in Se=C=Se. This is very encouraging. Table 4 shows only the highest level *ab initio* calculations compared with DFT calculations and experiment. Keeping in mind that the rovibrational corrections are about −60 ppm (i.e. σ_e may be converted into experimental σ_0 by adding −60 ppm), the CCSD values are within 3–5% of the experimental values. On the other hand, the DFT results are less shielded than the CCSD values by 100–200 ppm.

The situation for ^{125}Te is comparable to that in ^{77}Se. The ^{125}Te nucleus in TeF_6 gas has an absolute shielding of 2570 ± 130 ppm in the zero-density limit, if the nonrelativistic diamagnetic shielding of the free

Table 4 Calculated ^{77}Se shielding compared with experimental absolute shielding values in the gas phase (in ppm)

Molecule	H_2C=Se	Me_2Se	H_2Se	O=C=Se	Se=C=Se
CCSD σ_e[a]	−741	1877.5	2213	2345	1596
DFT σ_e[b]	—	1668	2093	2270	1441
Expt. σ_0[c]	-900 ± 200	1756 ± 64	2101 ± 64	2348 ± 60	1610 ± 80

[a]Gauss et al.[83]
[b]Ziegler et al.[84]
[c]See Jameson[85] for the original sources of the experimental data.

Encyclopedia of Analytical Chemistry, Online © 2006–2013 John Wiley & Sons, Ltd.

This article was published in the *Encyclopedia of Analytical Chemistry* in 2013 by John Wiley & Sons, Ltd.
DOI: 10.1002/9780470027318.a6109.pub2

atom is used. The DFT nonrelativistic calculations give 2260 ppm,[86] which is 200–300 ppm less shielded. This is in the same direction as the difference between DFT and CCSD in the ^{77}Se case. The ability of DFT calculations to reproduce the full range of ^{125}Te chemical shifts in all types of chemical bonding situations is encouraging.[86] Approximate relativistic calculations of ^{125}Te chemical shifts in the same set of molecules at the MP2 level give a better correlation with experiments (in solution), partly because spin orbit (SO) contributions are found to be non-negligible.[87] As an indication of how muddled the situation is for heavy nuclei, various calculations of the relativistic corrections for Te in TeH_2 lead to values from 861 to 1450 ppm, depending on the type of relativistic method used, electron correlation level, and basis set size. This is a considerable spread (589 ppm) in comparison to the spread in nonrelativistic values, which is 346 ppm. Clearly, results from different groups of calculations cannot be directly compared because systematic improvement in basis set size and level of electron correlation has not been carried out. Four-component calculations do not necessarily lead to more accurate results, because electron correlation level and basis set saturation issues are not yet settled.

Benchmark data and case studies for relativistic calculations for heavy nuclei are provided in the review by Autschbach and Zheng.[52] The spread in calculated values for benchmark systems such as HX (X = Cl, Br, I) is indicative. While nonrelativistic F shielding has a spread of 15.5 ppm, all values are within one sigma of the experimental absolute shielding value; on the other hand, for Cl, Br, and I, where relativistic methods are required, the spread is 95 ppm, 784 ppm, and 4571 ppm, respectively. The nonrelativistic values for Cl, Br, and I have a spread of only 60, 135, and 386 ppm; so although basis set quality may be inadequate and electron correlation treatments are not optimal, it can be deduced that relativistic corrections are by and large responsible for the incoherent nature of the calculated results for halogen nuclei.

For transition and post-transition metal nuclei, there are the usual problems associated with heavy nuclei (both scalar and SO relativistic contributions are expected to be important), plus the lack of absolute shielding information. In calculations for other transition and post-transition metal nuclei, only shielding differences, i.e. chemical shifts, have been used to compare with experiment. With one exception, there are no gas-phase data to compare with. There is the added complication that many measurements for transition metal nuclei are made in solutions of complex ions, where solvation effects can be very important. Despite these problems, some DFT calculations have been done for ^{103}Rh, ^{91}Zr, ^{57}Fe, and ^{59}Co. It is still an open question which type (hybrid, GGA, other) of exchange correlation functional would be best to use. The range of transition metal shifts is usually very large and these shifts exhibit useful diagnostic variations with ligand types, but the agreement is not yet at the level that is achievable routinely with ^{13}C shielding calculations. The theoretical calculations have yet to catch up with experiment. Witness, for example, the one case where gas-phase data are available: $CdMe_2$ molecule. Beam measurements show neat $CdMe_2$ liquid being deshielded by 1746 ppm from the free Cd atom, which has an absolute shielding of 4813 ppm. Thus, $\sigma = 3067$ ppm for neat $CdMe_2$ liquid at room temperature. The gas is found to be 62.1 ppm unusually less shielded than the neat liquid,[88] so that $\sigma = 3005$ ppm for gaseous $CdMe_2$ at 97°C. This is to be compared with 3504.5 ppm (too shielded by 500 ppm) from GIAO Cd shielding calculations on an isolated molecule of $CdMe_2$, with a spread of 105 ppm depending on the basis set used, neglecting relativistic corrections or electron correlation.[89] Other calculations give more shielded values than this, as much as 900 ppm more shielded than 3005 ppm. Since the chemical shift range of Cd is about 900 ppm, the achieved level of accuracy needs considerable improvement. A review of calculations for heavy nuclei by Autschbach and Zheng[52] provides insight and illustrative examples, particularly for very heavy nuclei such as Pb, Hg, and Au.

4 CALCULATIONS OF SPIN–SPIN COUPLING CONSTANTS

The various mechanisms in the nonrelativistic limit, given by Equations (10)–(14) are $\mathbf{J}^{(OD)}$, $\mathbf{J}^{(OP)}$, $\mathbf{J}^{(FC)}$, $\mathbf{J}^{(SD)}$, and the cross-term $\mathbf{J}^{(SDFC)}$, which has no isotropic part. The OD term, $\mathbf{J}^{(OD)}$, is the only term that is not expressed as an SOS in the Ramsey formulation, rather it is an average value of an operator containing two nuclear spins. $\mathbf{J}^{(OD)}$ is not usually small and can be rather large for ^2J(HH). A systematic study of this term shows that it is not very sensitive to basis set choice (double zeta with polarization functions are sufficient) and to inclusion of electronic correlation (SCF average values will do); this term is particularly important for ^nJ(HH), independent of n. The sign of the contribution is negative for two-bond HH coupling. From a systematic study of the OP mechanism using DFT, $\mathbf{J}^{(OP)}$ appears to be significant for most couplings although not dominant, and is particularly important for couplings involving a nucleus with lone pairs. The sign of the contribution (reduced so as to not include the nuclear gamma values) can be positive or negative; $\mathbf{J}^{(OP)}$ is negative and is the largest contribution for CO and N_2 molecules, for example. The SD term $\mathbf{J}^{(SD)}$ is the most time-consuming to calculate and so is

Encyclopedia of Analytical Chemistry, Online © 2006–2013 John Wiley & Sons, Ltd.

This article was published in the *Encyclopedia of Analytical Chemistry* in 2013 by John Wiley & Sons, Ltd.
DOI: 10.1002/9780470027318.a6109.pub2

sometimes neglected; it is not small when multiple bonds are involved between the coupled nuclei. For example, for N_2 molecule it is comparable to and partly cancels the $\mathbf{J}^{(FC)}$ term.[90] Electron correlation is very important for multiple bonded systems and for nuclei with lone pairs and must be accounted for, to obtain reliable results. Results at the SCF level have the wrong sign and magnitudes for coupling in both CO and N_2 molecules; the magnitudes are completely off for couplings in $H_2C{=}CH_2$, whereas correlated *ab initio* methods (CASSCF, SOPPA, CCSD) give very good values and the correct signs compared to experiment, with CCSD being the best. Gauss suggests that only the unrelaxed CC3 approach appears to be a suitable scheme for the general and reliable calculation of **J** with an approximate inclusion of triple excitations, as CCSD(T) suffers from problems due to triplet instabilities or near instabilities and cannot be recommended for this purpose.[91]

DFT calculations have difficulty reproducing the results for CO and N_2, regardless of the functional used, and the popular functionals do more or less about the same, in signs and magnitudes for the one-bond *J* between first-row nuclei and for all the couplings in $H_2C{=}CH_2$.

The sign and magnitude of the FC term, $\mathbf{J}^{(FC)}$, term (reduced) varies across the periodic table. Where no multiple bonds are involved, this mechanism usually provides the largest contribution to one-bond coupling constants. Electron correlation is very important for this mechanism and unrealistic values may result from calculations at the SCF level. The comprehensive review by Helgaker et al.[92] of theoretical methods for calculating spin–spin coupling *J* tensors includes comparisons of results using different levels of theory, different methods of including electron correlation and relativistic effects, as well as applications in the solid state.

4.1 One-Bond Coupling Constants

Table 5 shows the various contributions to the one-bond couplings in HF, HCl, CO, and N_2. The uncorrelated results (RPA) are shown to be inadequate. Among the various methods of including electron correlation, SOPPA, CCSD, MBPT, MCLR theory, and DFT, the DFT calculations suffer from the inadequacy of the functionals, which may be good enough to reproduce binding energies, but offer less accurate descriptions of the electron spin distributions where they are needed in calculations of **J**, especially the FC mechanism. As seen in Table 5, DFT gives the worst results among the correlated calculations. MCLR theory uses an MCSCF reference state and is capable of describing electronic systems with large static correlation effects.

How well do calculations predict the simple one-bond ^1J(CH)? Here the isotropic value is found to be entirely dominated by the FC mechanism and is easily reproduced by calculations that include correlation, including DFT. Correlation effects can be substantial. For example, the uncorrelated calculation of the FC term for ^1J(CH) in HCCH molecule leads to 449.3 Hz, whereas SOPPA, which includes correlation up to second order gives 246.5 Hz, which agrees quite well with the experimental value of 248.7 Hz. On the other hand, calculations are

Table 5 One-bond spin–spin coupling constants (Hz)

Molecule	Method	References	$\mathbf{J}^{(FC)}$	$\mathbf{J}^{(OP)}$	$\mathbf{J}^{(OD)}$	$\mathbf{J}^{(SD)}$	J	**J** (Expt.)
HF	RPA	93	467.3	119.3	−0.1	−12.4	654.1	—
	SOPPA	93	338.3	195.7	−0.1	−1.0	532.9	—
	MBPT	94	390.71	195.14	1.69	−17.47	570.01	—
	DFT	95	198.1	198.0	0.1		396.2	—
	CCSD	21	338.2	176.2	0.0	−1.0	513.4	529 ± 23
$H^{35}Cl$	RPA	21	16.78	13.70	0.00	−0.45	30.03	—
	MBPT	94	12.52	12.02	0.00	−0.08	24.45	—
	CCSD	21	22.04	12.65	0.00	0.34	35.03	37.7
$^{13}C^{17}O$	RPA	96	−8.1	12.2	0.1	−9.3	−5.1	—
	SOPPA	96	7.3	14.8	0.0	−4.0	18.1	—
	MCLR	90	6.69	13.66	0.09	−4.33	16.11	—
	DFT	95	13.4	12.4	0.1	—	25.9	—
	CCSD	21	7.0	13.0	0.1	−4.6	15.5	—
	CC3	91	6.92	13.1	0.1	−4.82	15.30	16.4 ± 0.1
$^{14}N^{15}N$	RPA	96	−7.65	0.50	0.0	−8.13	−15.26	—
	SOPPA	96	0.45	3.25	0.0	−1.55	2.18	—
	MCLR	90	−0.23	2.83	0.02	−1.85	0.77	—
	DFT	95	2.0	2.7	0.0	—	4.7	—
	CCSD	21	0.3	2.8	0.02	−1.7	1.4	—
	CC3	91	0.80	2.78	0.03	−1.84	1.77	1.8 ± 0.6

Encyclopedia of Analytical Chemistry, Online © 2006–2013 John Wiley & Sons, Ltd.

This article was published in the *Encyclopedia of Analytical Chemistry* in 2013 by John Wiley & Sons, Ltd.
DOI: 10.1002/9780470027318.a6109.pub2

Table 6 Contributions to the calculated anisotropy of the one-bond coupling in HX molecules, $\Delta\mathbf{J} = (\mathbf{J}_{||} - \mathbf{J}_{\perp})$ (Hz)[a]

		$\mathbf{J}^{(FC)}$	$\mathbf{J}^{(OD)}$	$\mathbf{J}^{(OP)}$	$\mathbf{J}^{(SD)}$	$\mathbf{J}^{(SDFC)}$	Total
HF, SCF	$\mathbf{J}_{||}$	453.44	143.50	−11.34	−71.96	−392.22	121.41
	$\mathbf{J}_{\perp}$	453.44	−69.43	297.82	0.44	196.11	878.38
	$\Delta\mathbf{J}$	0	212.93	−309.16	−72.4	−588.33	−756.97
HF, MBPT(2)	$\mathbf{J}_{||}$	390.71	143.12	−8.92	−58.78	−373.40	92.73
	$\mathbf{J}_{\perp}$	390.71	−69.03	297.17	3.18	186.63	808.65
	$\Delta\mathbf{J}$	0	212.15	−306.09	−61.96	−560.03	−715.92
HCl, SCF	$\mathbf{J}_{||}$	25.17	13.19	−2.90	−2.33	−42.26	−9.14
	$\mathbf{J}_{\perp}$	25.17	−6.60	18.95	0.71	21.13	59.36
	$\Delta\mathbf{J}$	0	19.79	−21.85	−3.04	−63.39	−68.50
HCl, MBPT(2)	$\mathbf{J}_{||}$	12.52	13.19	−2.52	−1.84	−41.38	−20.03
	$\mathbf{J}_{\perp}$	12.52	−6.59	19.29	0.80	20.68	46.70
	$\Delta\mathbf{J}$	0	19.78	−21.81	−2.64	−62.06	−66.73

[a]Fukui et al.94

less successful with the one-bond ^1J(CF). DFT is found to underestimate the FC contribution to the one-bond coupling because of the inability of existing exchange correlation functionals to produce the accurate spin densities required for this calculation. In the presence of polarizable lone pairs, the correlation problem is more severe, and the available functionals do not describe the spin densities well enough in the case of ^1J(CF), which are predicted by DFT to be about 100 Hz away from experimental values in every case.

There are many interesting trends observed in coupling constants, in signs, magnitudes, dependence on substituents, stereochemistry, position of coupled nuclei in the periodic table, and so on.[97] Many of these trends have been very useful in analysis of spectra, and yet a sound theoretical basis for few of such trends has been established.

The anisotropy of the tensors calculated with and without electron correlation are shown in Table 6 for HF and HCl.[94] First of all, note that the FC mechanism is purely isotropic and the cross-term $\mathbf{J}^{(SDFC)}$ which has no isotropic part, is responsible for a large part of the total anisotropy of the tensor. The anisotropy of the orbital mechanisms are opposite in sign and partly canceling. The contribution to the anisotropy from the SD mechanism is itself small. Any anisotropy observed in the **J** tensor in oriented molecules has to come from the mechanisms other than the FC term. However, because of the very large contribution from the cross-term $\mathbf{J}^{(SDFC)}$ to the anisotropy (78% in HF and 93% in HCl), the magnitude of the measured anisotropy unfortunately conveys very little information about the magnitude of the contributions of mechanisms other than the FC term to the isotropic average observed in solution. The effect of electron correlation on the individual components of $\mathbf{J}^{(OD)}$ is small. (It is well known that the effect of correlation on the isotropic average of $\mathbf{J}^{(OD)}$ is small and that it is not very sensitive to basis set choice.) The orbital mechanisms have opposite contributions to the anisotropy, $\mathbf{J}_{||}^{(OD)}$ and $\mathbf{J}_{\perp}^{(OP)}$ are similar in sign (positive) and magnitude (large), and so are $\mathbf{J}_{||}^{(OP)}$ and $\mathbf{J}_{\perp}^{(OD)}$ (negative and smaller). The effect of electron correlation on the cross-term $\mathbf{J}^{(SDFC)}$ is about 5%. If this is typical, uncorrelated calculations should permit estimation of the **J** anisotropy that may be expected in oriented systems. There are only a few measurements of the anisotropy of the **J** tensor because the observable quantity in solids is the $(\mathbf{D} + \mathbf{J})$ tensor, and the direct dipolar coupling tensor **D** overwhelms the sum. The anisotropy of the **J** tensor has been determined in a few favorable cases, such as $^1J(^{31}\mathrm{PX})$, where $\mathrm{X} = {}^{199}\mathrm{Hg}$, $^{95}\mathrm{Pt}$, $^{115}\mathrm{In}$, in Wasylishen's laboratory.[98] A typical measurement of this type in a single crystal of a mercury phosphine complex shows the experimental technique for arriving at $\mathbf{J}_{||} = 11\ 800$ Hz, $J_{\perp} = 6400$ Hz, and the isotropic value is 8200 Hz. While the isotropic value is very likely to be dominated by the FC mechanism, the anisotropy $\Delta\mathbf{J} = 5400$ Hz comes entirely from the non-FC mechanisms.[98]

MCSCF calculations of a wider set of diatomic molecules in addition to HF and HCl, (LiH, LiF, NaF, KF, Na2, NaK, BF, AlF, ClF) by Bryce and Wasylishen[99] reveal trends in anisotropy arising from the various mechanisms with position of coupled nuclei in the periodic table. It is interesting to find that the anisotropy in *J*-coupling can be large compared to the direct dipolar coupling, and that the anisotropy can be as large as 2.5 times the isotropic *J* that is observed in solution.

4.2 The Two-Bond Coupling Constant

The geminal coupling constant ^2J(HH) turns out to be very difficult to predict. As is the case for all ^nJ(HH), the $\mathbf{J}^{(OD)}$ term is important. So also is the $\mathbf{J}^{(OP)}$ term, but it has the opposite sign to the $\mathbf{J}^{(OD)}$ term. For the series CH_4,

Encyclopedia of Analytical Chemistry, Online © 2006–2013 John Wiley & Sons, Ltd.

This article was published in the *Encyclopedia of Analytical Chemistry* in 2013 by John Wiley & Sons, Ltd.
DOI: 10.1002/9780470027318.a6109.pub2

SiH_4, GeH_4, SnH_4, the orbital mechanism $\mathbf{J}^{(OD)}$ and $\mathbf{J}^{(OP)}$ terms have opposite signs and they very nearly cancel in CH_4. The magnitude of the $\mathbf{J}^{(FC)}$ term varies from large negative to large positive. There is poor agreement of the total calculated value with experiment.[22] The experimental variation of ^2J(HH) with the nature of the intervening atom is not predicted quantitatively, although the trend of algebraically increasing from C to Sn is reproduced at every level of correlation treatment.[22,92] In the series CH_4, NH_3, OH_2, ^2J(HH) has the sign of the $\mathbf{J}^{(FC)}$ term, but is by no means dominated by it. Here too, the experimental variation of ^2J(HH) with the position of the intervening atom in the periodic table is not predicted quantitatively, although the trend of algebraically increasing from C to N to O is reproduced at every level of correlation treatment.[21]

4.3 Coupling Over Three Bonds

From a practical viewpoint, one of the very early major successes of theoretical calculations of spin–spin couplings is the prediction of the torsion angle dependence of ^3J(HCCH), known as the *Karplus equation*. The very simple valence bond calculation[100] using a small four-atom fragment (HCCH) led to an unequivocal prediction which permitted a practical determination of structure strictly from the observed isotropic value of the coupling constant. It was found later that the dihedral angle dependence of the three-bond coupling is very general and Karplus-type equations have been used to describe many types of three-bond coupling pathways, for example ^3J(X–Y–C–H), where X represents other nuclei such as ^{31}P, ^{13}C, or ^{15}N, and three-bond coupling paths such as PtCCC, PWNN, PCPSe, etc. Used with caution, experimental ^3J values and a Karplus equation make a reasonable conformational probe. The original Karplus equation is written in the form of Equation (19)

$$^3J(\mathrm{HCCH}) = C_0 + C_1 cos\phi + C_2 \cos(2\phi) \qquad (19)$$

with $C_0 = 8.02$, $C_1 = -1.2$, and $C_2 = 7.0$ Hz as the empirical parameters, although other forms have also been used. The coefficients in the above equation have been calculated by various methods using ethane as the model. The $\mathbf{J}^{(FC)}$ contribution is the largest and $\mathbf{J}^{(SD)}$ the smallest. One such calculation, with second-order correlation for all contributions except the FC contribution (which was done with third-order correlation), leads to $C_0 = 4.66$, $C_1 = 0.39$, and $C_2 = 5.78$ Hz.[101] In the general case, the ^3J value also depends on the bond angles between any two adjacent bonds out of the three, and there are substituent effects. It is recommended that Bayesian analysis be used to find the appropriate parameters for a particular structure type: proteins, sugars, etc. Bayesian analysis of the coupling data in ubiquitin provides the parameters for Karplus type equations for $^3J(C'–C')$, $^3J(C'–H^\alpha)$, $^3J(C'–C^\beta)$, $^3J(H^N–C')$, $^3J(H^N–H^\alpha)$ and $^3J(H^N–C^\beta)$ without any bias.[102] The analysis is based on the notion that the observation of a scalar coupling constant of strength ^3J is described through a probability expressing the fact that, owing to experimental and processing errors as well as theoretical shortcomings measured and theoretically predicted, scalar couplings will never match exactly. Assuming no systematic deviation, a Gaussian error model is used.

4.4 Relativistic Effects

Why are relativistic effects important for spin–spin couplings of heavy nuclei? Relativistic effects are particularly important for electronic properties that depend on the electronic wavefunctions very close to nuclei where electrons move fast. Relativistic effects on the electronic structure of atoms and molecules consist of a contraction of s and p shells, the spin–orbit splitting of the non-s shells, and the relativistic SCF expansion of d and f shells. The contraction of the s and p shells leads to larger spin densities at the nuclei (FC term) and also larger values of $\langle r_{kN}{}^{-3}\rangle$ (other mechanisms). An *a posteriori* correction of the nonrelativistic values of these by a multiplicative factor $B(n, Z)$, depending on the principal quantum number n and the nuclear charge Z, was suggested by Breit in 1930,[103] and this multiplicative factor has been used by Pyykkö et al.[104] to impose a simple relativistic correction on the values of J calculated using the nonrelativistic formulas. This factor, $B(n, Z)$, is 1.348 for the $n = 5$ shell of Sn and is 2.592 for the $n = 6$ shell of Pb. This means the nonrelativistic calculations underestimate the value of J(SnH) by a factor of 1.348. When both nuclei involved in the coupling are heavy, the product of two such factors is substantial.

Experimental measurements on diatomic molecules in the gas phase provide excellent tests for computational methods, especially when the data provides the anisotropy of the $\mathbf{J}$ tensor. Relativistic hybrid DFT calculation of indirect nuclear spin–spin coupling tensors were compared with experiment for diatomic halides MX, M = (Li, Na, K, Rb, Cs), X = (F, Cl, Br, I) and for polyatomic xenon fluorides and group-17 fluorides.[105] The relativistic (two-component ZORA formalism including scalar and spin–orbit corrections) DFT (hybrid functional PBE0, which includes 25% exact exchange) calculations reproduce the anisotropy of the coupling constant very well. For some of the heaviest molecules in the set, the relativistic effects coming from spin–orbit coupling can be quite large compared to the scalar part. Figure 3 shows the quality of the results from the relativistic DFT calculations of the isotropic

Encyclopedia of Analytical Chemistry, Online © 2006–2013 John Wiley & Sons, Ltd.

This article was published in the *Encyclopedia of Analytical Chemistry* in 2013 by John Wiley & Sons, Ltd.
DOI: 10.1002/9780470027318.a6109.pub2

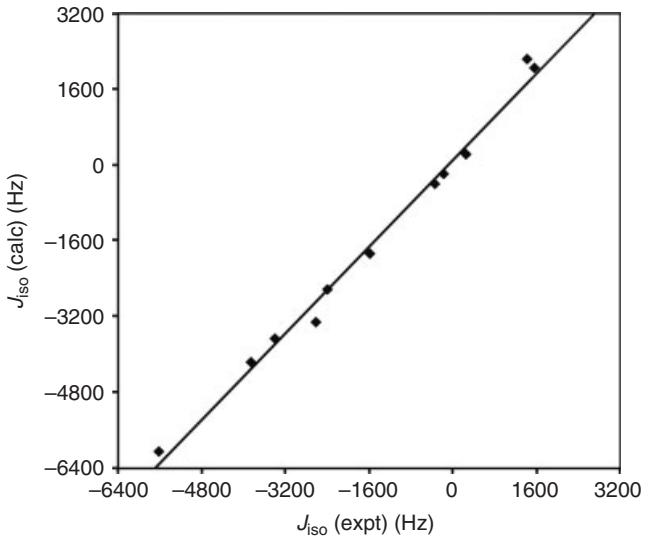

Figure 3 Plot of calculated isotropic coupling constants versus experimental values for the group-17 fluorides and xenon fluorides. The calculated values are ZORA at spin–orbit level using the PBE0 functional that includes 25% exact exchange. (Reproduced from Ref. 105. © 2009 Canadian Science Publishing or its licensors. Reproduced with permission)

part of **J** for polyatomic xenon fluorides and group-17 fluorides. Earlier studies of **J** in interhalogen diatomic molecules using the same relativistic formalism but with the GGA functional also showed excellent agreement with experiment for both the anisotropy and the isotropic value. In addition a good linear correlation was found for the anisotropy and the isotropic value of the coupling constant (with the γ of the nuclei divided out) against the product of the atomic numbers of the coupled nuclei.

5 CALCULATIONS OF ELECTRIC FIELD GRADIENTS

5.1 Calculations of Electric Field Gradients at Nuclei in Isolated Small Molecules

Since it is the coupling of the nuclear electric quadrupole moment with the EFG that is observed in experiments, it is necessary and sufficient to know either one of them to determine the other from spectroscopic data. The most reliable method of obtaining the intrinsic electric quadrupole moment of a nucleus is by very high-quality *ab initio* calculations of the EFG tensor in selected small molecules in which the nuclear quadrupole couplings of the nucleus have been measured accurately via microwave spectroscopy. The value of eQ, a property of the bare nucleus, is obtained as a fit parameter. Once calibrated, this eQ value is used to deduce from experiment the EFG tensor for any other nuclear site of the nucleus. Tables of eQ values continue to be refined with emergence of quantum mechanical EFG calculations of increasing accuracy, including vibrational corrections.

Accurate theoretical calculations of EFGs for small molecules pose no special problems; requirements of basis set quality and appropriate level of electron correlation depend on the molecule, just as for calculations of shielding, but less demanding in that only the ground electronic wavefunction is required. Just as for shielding calculations, the r^{-3} factor in the EFG requires wavefunctions that are accurate in the immediate vicinity of the nucleus.

5.2 Simulations of Nuclear Quadrupole Coupling in Associated Liquids

The presence of neighboring molecules influences the EFG at a nuclear site, by directly providing additional charge distributions outside of the molecule and also by distorting the electronic distribution of the molecule of interest. An extreme case is a liquid in which hydrogen bonding or complex formation is present. One approach to the calculation is to consider the liquid as having a distribution of clusters of all sizes, monomers, dimers, n-mers where n is truncated at some value when the contribution to the average value is sufficiently small. Molecular geometries of each n-mer are optimized and the EFGs are calculated at each nuclear site in the n-mer. Molecular partition functions are calculated for each n-mer, and from thermodynamic calculations, the distributions of the n-mers are obtained. The average EFG for each cluster is weighted with the cluster distribution to obtain the EFG values in the liquid phase. The ^{14}N, ^{17}O, and ^{2}H of the carbonyl and *cis* and *trans* amides have been calculated in liquid formamide by this method, for comparison with the experimental values of NMR quadrupolar relaxation time as a function of temperature.[106] Cyclic hexamers are found to be the dominant species at room temperature, consistent with structural data from neutron diffraction, low-frequency Raman, and far-infrared spectra. This method of calculation has been applied to liquid HCN, in which the calculated values for the isolated monomer, dimer, and trimer successfully predict the values known independently from pulsed Fourier transform microwave experiments on the van der Waals complexes.[107] Theoretical calculations such as these, combined with measurements of the nuclear quadrupole coupling constants as a function of temperature, can provide a useful general probe of electronic changes accompanying hydrogen bonding, cluster formation, solvation, phase condensation, and other phenomena in condensed media.

Encyclopedia of Analytical Chemistry, Online © 2006–2013 John Wiley & Sons, Ltd.

This article was published in the *Encyclopedia of Analytical Chemistry* in 2013 by John Wiley & Sons, Ltd.
DOI: 10.1002/9780470027318.a6109.pub2

5.3 Electric Field Gradient Tensor and Electronic Structure in the Solid State

Calculations offer a systematic way to investigate the dependence of NMR parameters, particularly the EFG, on structure in the solid state. Bond distances, bond angles or neighbor atoms can be varied much more easily than in an experiment. The EFG tensor is intimately related to the local molecular structure. In crystalline silicates, for example, the measured ^{17}O nuclear quadrupole coupling constant serves as a probe of oxygen coordination number and geometry. Using experimental correlations between structure (e.g. Si–O–Si bond angles) in crystalline silicates and the measured ^{17}O quadrupolar coupling constants, the Si–O–Si bond angle distribution in silicate glasses can be deduced, bridging and nonbridging oxygens can be distinguished.[108,109] Although particularly useful in inorganic chemistry,[110] structure determination of biomaterials can also be elucidated by EFG tensors of ^{14}N, ^{17}O, ^{2}H, as well as metal ions such as Ca^{2+}, which are naturally occurring in such systems. EFG tensors of deuterium nuclei in hydrogen-bonded positions, such as the amide or carboxy hydrogen in peptides, give deuteron/proton bond directions with an accuracy rivaled only by neutron diffraction, as it has been established that the unique eigenvector of a deuteron quadrupole coupling tensor is approximately parallel to the bond direction of the deuteron. ^{14}N EFG tensor is shown to be highly sensitive to the surrounding environment, particularly to nearby hydrogen bonding in a study of N EFG tensors in crystalline amino acids.[111] An analysis of the EFG for a variety of typical structural motifs can provide an intuitive way of understanding the chemical origin of the magnitude and the sign of EFG tensors at nuclei, as well as of their orientation with respect to the molecular coordinate frame. This is provided in a lucid treatise in chemical structural terms by Autschbach et al.[112]

For practical solid-state calculations using GIPAW, for example, a prerequisite is an initial structure, typically obtained from diffraction experiments. When the quality of such data is insufficient (locations of light atoms such as H are not specified, or only a low-resolution structure is available), geometry optimization is required prior to making calculations of NMR parameters. On the other hand, when single-crystal data are available from synchrotron measurements or neutron diffraction, very little change of the NMR parameters occurs upon geometry optimization.

5.4 Relation Between Chemical Shift and Electric Field Gradient Tensors in the Solid State

NMR measurements in single crystals permit the independent determination of the principal axis systems of the EFG tensor and the shielding tensor. Even in the powder it may be possible to find the relative orientation of these two axis systems by referring to the known axis system for the dipolar coupling. The two axis systems are not necessarily coincident. Theoretical calculations of both the EFG and the shielding tensors at the same nuclear site provide descriptions of the electronic distribution and chemical bonding that can be checked directly against experiment. They provide respectively, a measure of the bond direction and the strength of the hydrogen bond for the deuterium nucleus, for example. In materials that exhibit a distribution of nuclear sites, such as glasses or polymers, multidimensional solid-state NMR techniques permit the determination of the anisotropic chemical shift as a function of the isotropic chemical shift or of the EFG as a function of the isotropic chemical shift. From such measurements, the anisotropic chemical shift of ^{29}Si and the EFG of ^{17}O nuclei, for example, can both be used to characterize a silicate glass or other complex materials, providing complementary information. Thus, these two tensors provide local electronic information even in complex materials. With the assistance of theoretical calculations, such multidimensional solid-state NMR experiments can provide answers to questions about the microscopic structure of solids, on the extent of order/disorder in cation environments, random distributions or amorphous/crystalline domains, short-range and long-range order, and so on.

5.5 Relativistic Effects on Electric Field Gradients

In four-component variational relativistic quantum chemical methods, the electronic contribution to the EFG is calculated as an integral over the electron charge density distribution multiplied with the field-gradient operator. With the four-component method, both the scalar and spin–orbit effects are included, and accurate calculations are carried out with large basis sets and a high level of electron correlation, for example CCSD(T). MP2 may not be sufficient. The benchmark set of molecules is once again HX, (X = F, Cl, Br, I),[113] and also Hg in its compounds.[50] Two-component calculations have also been carried out on the same HX set, and further application to group-13 iodides and uranyl ions,[44] or Hg in its compounds,[114] with high accuracy.

In the solid state, for the calculation of properties with a large contribution in the region close to the nucleus, it is necessary to use projected augmented wave (PAW) operators modified to account for relativistic effects. Yates et al.[59] have used GIPAW operators modified using the ZORA to compute ^{77}Se and ^{125}Te shieldings. It remains to be seen how much the calculation of solid-state NMR spectra of heavy quadrupolar nuclei

Encyclopedia of Analytical Chemistry, Online © 2006–2013 John Wiley & Sons, Ltd.

This article was published in the *Encyclopedia of Analytical Chemistry* in 2013 by John Wiley & Sons, Ltd.
DOI: 10.1002/9780470027318.a6109.pub2

will be dependent on relativistic effects. An unusual finding for the ^{127}I EFG tensors in MgI_2, CaI_2, SrI_2, and BaI_2 solids: from the very good agreement between the experimental and the computed values it has been suggested that relativistic contributions appear to be minimal for EFG at the I nucleus in these particular systems.[115]

6 INFLUENCE OF INTRAMOLECULAR GEOMETRY AND ENVIRONMENT ON NUCLEAR MAGNETIC RESONANCE PARAMETERS

The temperature dependence, mass dependence (isotope effects), and site sensitivity (e.g. dependence on secondary/tertiary structure of proteins) of chemical shifts, spin–spin couplings, and EFGs provide very useful additional information about structure, dynamics, and environment of a molecule or a particular part of a molecule, that is not available from other experiments.

6.1 Nuclear Magnetic Resonance Parameter Dependence on Local Geometry: Bond Lengths, Bond Angles, Torsion Angles

The insight into structure and environment provided by the NMR chemical shift is obtained by a combination of theoretical calculations and experiments.[116] The NMR chemical shift discriminates between the various alanine residues in the same protein molecule, between two nuclear sites identical in every way except that one has ^{18}O in a neighboring bond rather than ^{16}O (isotope shift studies), between a ^{15}N (and ^{13}C) in a dynamically averaged rather than rigid headgroup at an oriented membrane interface, for example. In most cases, theoretical calculations using innovative model fragment systems are required to interpret the relation between the structure and the chemical shift. The discrimination is afforded by the extreme sensitivity of the shielding tensor to the local geometry: the bond lengths, bond angles, and torsion angles. The mathematical surface describing the shielding tensor as a function of these geometrical parameters is called a *shielding surface*. Vibrational averaging over the shielding surface, weighted by the probabilities of finding the molecule at the geometries described by these parameters (the vibrational wavefunction provides these probabilities) gives average shielding values that are different for different isotopomers, and average shielding values that are different for particular (ϕ, ψ) torsion angles that characterize particular alanine residues in a protein. Thus, isotope effects on chemical shifts can be predicted; the distinguishing chemical shifts of different alanine residues in a protein can be associated with specific local conformations, leading to structure determination. The application of quantum mechanical calculations of shielding surfaces to the structural characterization of proteins was introduced by de Dios et al.[117] This approach has led to the possibility of secondary and tertiary protein structure determination from NMR chemical shifts in solution using ^{13}C alone.[118] The method is extremely powerful when combined with complementary information obtained from geometry sensitivity of other NMR parameters such as spin–spin coupling and ^{1}H chemical shifts.[119] The use of theoretical calculations of NMR shielding surfaces to elucidate structure and dynamics finds application in the gas phase, in catalysis, as well as in biomolecular systems.[116,120,121]

This sensitivity of NMR chemical shifts to bond angles, torsion angles, and nearest neighbors established by theoretical calculations by de Dios et al. has been exploited in an empirical way by several groups. Bax et al.[122] developed a robust protocol for *de novo* protein structure generation, called *CS-ROSETTA*, using as input experimental parameters the $^{13}C^{\alpha}$, $^{13}C^{\beta}$, $^{13}C'$, ^{15}N, $^{1}H^{\alpha}$, and $^{1}H^{N}$ NMR chemical shifts alone. The protocol uses an empirically optimized procedure to select protein fragments from the Protein Data Bank, in conjunction with the standard ROSETTA Monte Carlo assembly and relaxation methods. CS-ROSETTA has been successfully applied in a blind manner to several protein targets with molecular masses up to 15.4 kDa, whose conventional NMR structure determination was done in parallel. CS23D2.0 is a web server set up by Wishart et al.[123] for rapidly generating accurate three-dimensional protein structures using only assigned NMR chemical shifts as input. It uses a combination of maximal subfragment assembly, chemical shift threading, shift-based torsion angle prediction, and chemical shift refinement to generate and refine the protein coordinates. It has been found to successfully arrive at a protein structure 90% of the time, at 10^{-3}–10^{-4} times the time that CS-ROSETTA does. The newer version by Wishart's group, GeNMR, can predict even totally novel folds and handles protein complexes as well.[124] There are also commonly used methods for torsion-angles-from-chemical shifts only, such as TALOS+, DANGLE, and PREDITOR. All use empirical information from the data base of protein structures.

The dependence of the spin–spin coupling, the EFG, and other molecular electronic properties on bond lengths and bond angles, and the observations that are the experimental manifestation of this, are similar to that discussed above for shielding. The general theoretical basis for isotope effects and temperature dependence of these properties is the same. With the assumption of the

Encyclopedia of Analytical Chemistry, Online © 2006–2013 John Wiley & Sons, Ltd.

This article was published in the *Encyclopedia of Analytical Chemistry* in 2013 by John Wiley & Sons, Ltd.
DOI: 10.1002/9780470027318.a6109.pub2

Born–Oppenheimer separation of nuclear motion from electronic motion, the mathematical surface describing the dependence of **J** (or other) on the geometrical parameters (such as bond lengths) exists, just as does the potential energy surface of the molecule. Averaging on the property surface is carried out according to the probability of finding the molecule at various geometries, which in turn is determined by the vibrational wavefunctions corresponding to the potential energy surface.[125] Raynes et al.[126] have provided very good case studies of these effects on coupling constants in polyatomic molecules, including details of the theoretical surfaces, vibrational averaging, and experimental measurements of the temperature dependence of spin–spin coupling in the various isotopomers. More recently, a set of calculations of the effects of vibrational averaging on CC calculations of **J** for hydrocarbons such as acetylene, ethylene, and cyclopropane by Sneskov and Stanton[127] provides one of the first systematic benchmarks of zero-point vibrational contributions to spin–spin coupling constants in polyatomic molecules using the reliable CC theory. Two-bond CCH couplings are the most affected by vibrational averaging, the vibrational contribution varying from 8% (acetylene) to 32% (ethylene). By incorporating the vibrational averaging effects, the accuracy of the J(C–C) as compared to experiment is indeed remarkable. Vibrational corrections to **J**, calculated by DFT and other methods, have also been studied. Upon including vibrational corrections, the mean absolute errors and standard deviations in comparison to experimental values decrease for all methods except DFT/B3LYP. It is found that DFT fails badly for molecules containing fluorine, as already mentioned in Section 4.1.

Sometimes the vibrational averaging can involve large amplitudes, for example, the inversion mode in NH_3.[128] In this case, an accurate potential surface needs to be generated (in this case, at the CCSD(T) level). Pointwise **J** surfaces also have to be generated and fitted to a fourth-order power series in the internal coordinates; then a full variational treatment of the nuclear motion is used to carry out the averaging using the variational wavefunctions obtained from the potential surface. For ^{1}**J**(NH), the bending motion increases the absolute value, whereas the stretching motion decreases it, leading to substantial cancellation and an overall slight decrease. Without the proper treatment of the large amplitude inversion mode, the vibrational correction to the isotropic **J** is underestimated by 57%.

6.2 Intermolecular Effects and Averaging

NMR shielding is extremely sensitive to intermolecular effects. This sensitivity is manifested by the very large gas-to-liquid shifts (4.4 ppm for ^{1}H in H_2O, 19.5 ppm for ^{15}N in NH_3, 77 ppm for ^{31}P in P_4, 120 ppm for ^{77}Se in H_2Se, around 200 ppm for ^{129}Xe in xenon), by the aromatic solvent-induced proton chemical shifts, and by the very large average chemical shifts observed for Xe in various media such as zeolites and polymers.[116,121] While the short-range effects (i.e. the geometry dependence and hydrogen bonding) on shielding of ^{13}C, ^{15}N, ^{17}O, and ^{1}H nuclei in each amino acid residue of a protein can be calculated using a model fragment including only the most immediate atoms to the nucleus of interest, the long-range effects of neighboring residues may be considered in the same way as intermolecular effects from solvent molecules. It has been found that such long-range electrostatic effects have an important role to play in interpreting ^{1}H, ^{15}N, and ^{17}O chemical shift inequivalencies in proteins, and neighbor anisotropy has an important role in the case of ^{1}H. The effects of hydrogen bonding on the ^{1}H shielding tensor in ice have been reproduced by calculations using 17 H_2O molecules arranged in the experimental ice configuration, for example, emphasizing the importance of long-range effects.[129]

Theoretical calculations of intermolecular effects are sometimes carried out by approximating the medium as a continuum and considering the molecule in a cavity within this medium of fixed dielectric constant. Such an option is routine in many quantum mechanical software packages. Another approach is to consider the intermolecular effects in terms of electrical polarization effects of fixed partial electrical charges centered on surrounding atoms in a crystalline system; the charge perturbation model was used to include the nonbonded contributions to shielding from remote atoms in the same protein molecule. Doing the quantum calculations in the presence of point charges adds trivially to the processing time without them. Of course, the preferred approach of including intermolecular effects in a crystal is by using a periodic boundary approach such as already described in Section 2.7.

When not in the solid state where dynamics is mostly vibrational, a nuclear site often suffers a dynamically changing contribution of intermolecular effects as the configurations of neighboring solvent or other neighbor atoms change within the time of observation associated with the NMR time scale. In such instances, in solution, in the neat liquid, or for nuclear sites experiencing exchange, intermolecular effects can only be taken into account properly by carrying out averaging over configurations or over time. The dynamic averaging may be carried out in various ways, but in general one needs (i) a means of generating configurations over which the averages are taken and (ii) a means of generating the shielding, **J**, or EFG for a given configuration, that is, one needs to quantum mechanically calculate

Encyclopedia of Analytical Chemistry, Online © 2006–2013 John Wiley & Sons, Ltd.

This article was published in the *Encyclopedia of Analytical Chemistry* in 2013 by John Wiley & Sons, Ltd.
DOI: 10.1002/9780470027318.a6109.pub2

the nuclear shielding or **J** or EFG in the molecule together with the solvent molecules at a very large number of internuclear separations and orientations, then one needs to average such shieldings (or **J** or EFG) over the appropriately weighted configurations at each temperature, by integrating the classical equations of motion [by a molecular dynamics (MD) trajectory], analytically integrating over configurations (this is only possible in simple cases, as in a dilute gas of simple molecules), or statistically sampling configurations in a smart way (as in Metropolis Monte Carlo) for canonical or grand canonical systems, whichever is appropriate. Depending on how strong the intermolecular interactions are, it may be necessary to do a fully quantum calculation, that is, include all the electrons and nuclei of the neighbors in each step of the motion by a quantum mechanical calculation (quantum MD). DFT is used in the latter approach as it is efficient for large numbers of electrons and nuclei, in a method developed by Car and Parinello, CPMD (molecular dynamics).

In order to save computational time, the shielding, **J**, or EFG at the nuclear site may have to be calculated with nonuniform accuracy among all atoms of the system. For example, the atoms closest to the nucleus of interest may be treated at a higher level of theory than the atoms farther out. A shell or onion type of structure to the space around the NMR nucleus arises where the innermost shell may be done quantum mechanically with correlated wavefunctions, while the outer shell may be done quantum mechanically at an SCF level or even at a molecular mechanics level. Many approaches to calculations in this type of shell structure can be used by Morokuma's ONIOM (our own *n*-layered integrated molecular orbital and molecular mechanics) method,[130] Karplus' QM/MM (quantum mechanics molecular mechanics) method,[131] or else by embedding the high-level quantum system in the remainder of the system, the latter treated as a collection of point charges self-consistently adjusted to provide the correct Madelung potential at the position of the nuclear site, an embedded ion model.[132]

One way to do the averaging is by MD, that is, to calculate the shielding (by any of the above-mentioned methods) for each of a set of configurations from an MD trajectory and do a simple average, each configuration weighted equally. MD has been used to produce a large number of instantaneous configurations for which the component magnitudes and directions of the ^{15}N shielding tensor can be calculated in a simple model system (three *N*-methylacetamide complexes) constructed from a gramicidin channel in a fully hydrated phospholipid bilayer.[133] The MD method of sampling reveals fluctuations in the tensor properties that may be used to investigate the types of NMR spectra produced during such motional averaging for a protein observed in a fluid bilayer environment.

Another means of generating configurations is by an importance sampling Monte Carlo method, in which the ensemble average of the quantity, for example, shielding, can be obtained with configurations generated according to their probability in a chosen distribution based on either energy (canonical ensemble) or chemical potential (grand canonical ensemble).[134] For the interpretation of distributions and chemical shifts of Xe atoms, periodic boundary condition grand canonical Monte Carlo simulations were carried out in various crystalline zeolites, aluminum phosphate, dipeptides, clathrate hydrates, and in constructed idealized crystalline materials containing paramagnetic centers. Here, precalculated Xe shielding surfaces were constructed from *ab initio* calculations using a large number of positions for the Xe atom within the cage, distributed according to the sharp dependence of the Xe shielding with distance from its neighbors. Neighbor atoms are included in the quantum calculation depending on the system. For clathrate hydrates, 40–48 water molecules surrounded the Xe atom and the remaining waters were represented by the embedded ion model. The shielding surfaces are found by mathematically fitting the *ab initio* results to appropriate functions so as to reproduce the *ab initio* shielding tensors from the fitted functions at arbitrary configurations. By using a pairwise additive approach for the shielding as well as for the interaction energy, the averaging can be carried out via importance sampling in a grand canonical Monte Carlo method.[56] The use of ^{129}Xe chemical shifts in studies of various electronic environments (zeolites, polymers, clays, coals, biological systems) depends on theoretical calculations of the intermolecular effects on ^{129}Xe shielding in the xenon atom. The dispersion of the Xe signal in these various media is very useful as a diagnostic tool in the analysis of structure of the medium, the distribution of Xe atoms within, and the rate of exchange (diffusion) of Xe from one cage (or channel or domain) to another, as well as from within the medium to the bulk phase. The ability to reproduce the temperature dependence of the intensities and the individual chemical shifts in the ^{129}Xe NMR spectrum of the various Xe_1, Xe_2, Xe_3, Xe_8 signals observed for xenon trapped in a variety of *A* zeolites, (Na*A*, $Ca_xNa_{12-2x}A$, K*A*, Ag*A*) using a combination of quantum mechanical calculations and statistical mechanical averaging, permits the interpretation of the NMR observations in various other zeolites wherein fast xenon exchange leads to one signal that contains the average over all distributions.[135] Xe chemical shifts are very large (several hundred ppm) and discriminate between amorphous and crystalline regions in polymers and coals; however, the theoretical prediction of the Xe

Encyclopedia of Analytical Chemistry, Online © 2006–2013 John Wiley & Sons, Ltd.

This article was published in the *Encyclopedia of Analytical Chemistry* in 2013 by John Wiley & Sons, Ltd.
DOI: 10.1002/9780470027318.a6109.pub2

NMR spectrum in these more complex materials lags behind the experiments. The same approach as used in the crystalline zeolites should work in these more complex systems, provided that an appropriate model system can be introduced and tested in each case. A review of the various theoretical approaches to dynamic averaging of chemical shifts in condensed phases provides a systematic classification and many examples from the literature.[56]

Theoretical approaches for intermolecular effects on **J** would be the same as for chemical shifts, although the observed effects are generally smaller. A counter example is provided by ^1J(N–H) and ^2J(H–H) in liquid ammonia.[136] Here the electric polarization effects of the rest of the molecules affect the *J*-coupling, as does the change in geometry while hydrogen bonding partners change orientation and distance. Thus, explicitly including hydrogen-bonded NH_3 molecules in the quantum calculations is essential, just as in the case of H_2O in liquid water. Here, QM/MM calculations of *J* (and shielding) were used with Monte Carlo averaging. Gas-to-liquid chemical shifts for ^{15}N and ^1H were also calculated, providing additional tests for the quality of the description of the system.

Intermolecular effects on EFGs at a nucleus can be substantial. In van der Waals dimers and higher *n*-mers, the nuclear quadrupole coupling tensor can be sufficiently different from that found in the monomer and can be used to deduce the structure of the clusters formed. Calculations of the EFG at a nucleus in a cluster treated as a supermolecule generally have to be carried out as a function of geometry, and it is usually necessary for internal coordinates to be permitted to vary with intermolecular separation. Furthermore, consistent with the strength of intermolecular forces, cluster vibrations can be very anharmonic, so averaging will have to be done accordingly. Farrar and Weinhold have carried out averaging of the EFG at the ^{14}N and ^2H nuclei of HCN in $(HCN)_2$, $(HCN)_3$, and $(HCN)_n$ up to $n = 6$.[107] The interpretation of the nuclear quadrupole couplings in liquid HCN as a function of temperature also requires that the distribution of the dominant clusters be calculated by statistical mechanics. The non-pairwise-additive cooperativity effects in hydrogen bonding that are comparable in magnitude to that of dimer formation in this system cannot be neglected in the calculation of the NMR parameters. For the same reason, the NMR parameters of liquid water or ice cannot possibly be deduced from calculations on the dimer $(H_2O)_2$ alone.

Including motional effects in the solid state is possible in analogous ways, by using Monte Carlo or MD and averaging the NMR parameters over the snapshots or by considering the vibrations of the atoms in the solid, even including temperature dependence of the dimensions of the unit cell itself.[137]

6.3 Calculations of NMR Parameters in Amorphous Solids

From the outset, Mauri's method was designed to be used not only for perfect crystalline solids but also for amorphous materials by using a 'supercell'. Structures that are inherently nonperiodic, e.g., surfaces, amorphous and disordered materials, may be studied theoretically with a large enough unit cell. With increasing computational resources, unit cells comprising many hundreds of atoms or encompassing large volumes can be used. By combining Monte Carlo or MD with GIPAW, it has been possible to interpret the NMR spectra of amorphous materials including vitreous silica, calcium, lithium, and sodium silicate glasses, as well as ceramics. An ensemble of glass models are obtained using MD simulations, geometry optimization is used to refine the structures, and then GIPAW is used to calculate the NMR parameters; the NMR lineshapes and multidimensional solid-state spectra can also be calculated from the results because complete tensor information for both shielding and EFG is available from GIPAW calculations. Disordered systems can require many calculations to be performed for different configurations of a model structure. The wide distribution of freely available and commercially available software using the GIPAW method for calculations of chemical shifts and EFGs has made it possible for chemists in the pharmaceutical industry to use solid-state NMR of cocrystals and amorphous solid dispersions to investigate these forms as alternatives to more established solid delivery forms, for example. The detailed structure of catalytic surfaces, such as hydroxy apatite and silica, has been investigated. Many more applications to the determination of local structure disorder and dynamics in the solid state may be found in the comprehensive review of chemists' application of GIPAW by Mauri et al.[137]

7 FUTURE DEVELOPMENTS

NMR parameters are extremely useful tools for studying structure, dynamics, and environment. Their usefulness is enhanced when measurements go hand in hand with calculations. Theoretical calculations of shielding, **J**, and EFG tensors for isolated small molecules are well in hand. Using a hierarchy of approximations, the exact solution may be approached systematically within CC theory, for example. Relativistic calculations can now be carried out in a theoretically rigorous manner with four-component wavefunctions but only for small systems.

Encyclopedia of Analytical Chemistry, Online © 2006–2013 John Wiley & Sons, Ltd.

This article was published in the *Encyclopedia of Analytical Chemistry* in 2013 by John Wiley & Sons, Ltd.
DOI: 10.1002/9780470027318.a6109.pub2

Most calculations of NMR parameters are nowadays carried out using DFT in larger isolated molecules, in MD simulations in solutions, and in the solid state. This is the most cost-effective method for calculations in larger systems. In applications of DFT, the most important choice is that of the exchange–correlation functionals. However, no single functional currently exists that is capable of providing reliable results for all properties for all systems, or even the same property for all systems. As we have seen, on using benchmark calculations of high accuracy for a specific set of molecules, different exchange–correlation functionals for different systems can be found to perform somewhat better than others, but none do as well as the accurate CC methods.[36] We have seen that in comparison to the accurate *ab initio* calculations, none of the existing functionals give sufficiently accurate results for NMR parameters. There are additional difficulties associated with DFT calculations of NMR parameters: the commonly used functionals are known to provide a poor description of the energetics of weak intra- and intermolecular bonds. This can result in dramatic unit cell expansions in solid-state calculations and unrealistic structures in unconstrained geometry optimizations of weakly bound and flexible systems. It is precisely in these cases that DFT is the method that is used, as it would be prohibitive to do coupled-cluster calculations of a large number of configurations when studying dynamic and disordered systems. The search for a more accurate approximation for the exchange correlation functional is still ongoing. This is probably the most important development for the future. Heavy nuclei, particularly transition metal nuclei, which are important components of technologically important solid materials, cannot be treated accurately until the problem of more accurate functionals is solved.

The extreme sensitivity of shielding and EFG tensors to intermolecular effects and local geometries (imposed by longer range order and distributions) presents a distinct advantage as well as difficulties for the use of NMR as an analytical tool. Applications of calculations of shielding and EFGs to interpretations and analyses of complex systems require construction of appropriate useful models that can be tested in simpler systems and extended to complex ones. Since the various components, short-range (geometrical, hydrogen bonding) and long-range intermolecular contributions vary from system to system, each system to be analyzed requires its own model. Theoretical calculations of spin–spin coupling constants are more difficult, even in isolated small molecules, but are slowly becoming more tractable. These have sensitivity to local geometries but are less susceptible to intermolecular effects and long-range contributions. Here too, the availability of more accurate exchange correlation functionals would make a significant difference.

ABBREVIATIONS AND ACRONYMS

B3LYP	Becke, three-parameter, Lee–Yang–Parr
BDFT	Magnetic Field Density Functional Theory
BLYP	Becke–Lee–Yang–Parr
CAS	Complete Active Spaces
CC	Coupled Cluster
CCSD(T)	Coupled Cluster Singles and Doubles
CDFT	Current Density Functional Theory
CPMD	Car and Parinello, Molecular Dynamics
CSGT	Continuous Set of Gauge Transformations
DFT	Density Functional Theory
EFG	Electric Field Gradient
FC	Fermi Contact
FCI	Full Configuration Interaction
GGA	General Gradient Approximation
GIAO	Gauge-including Atomic Orbital
GIPAW	Gauge-including Projected Augmented Wave
HALA	Heavy Atom on Light Atom
HRPA	Higher Random Phase Approximation
IGAIM	Individual Gauges for Atoms in Molecules
IGLO	Individual Gauge for Localized Orbitals
KSDFT	Kohn–Sham Density Functional Theory
LDA	Local Density Approximation
LORG	Localized Orbital/Local Origin
MAS	Magic-angle Spinning
MBPT	Many Body Perturbation Theory
MCIGLO	Multiconfiguration Individual Gauge for Localized Orbitals
MCLR	Multiconfiguration Linear Response
MCSCF	Multiconfiguration Self-consistent Field
MD	Molecular Dynamics
MP	Møller–Plesset
NMR	Nuclear Magnetic Resonance
NOE	Nuclear Overhauser Effect
OD	Diamagnetic Orbital
ONIOM	Our Own *n*-layered Integrated Molecular Orbital And Molecular Mechanics
OP	Paramagnetic Orbital
PAW	Projected Augmented Wave
PBE0	Perdew–Burke–Ernzerhof Hybrid
ppm	Parts per Million
QM/MM	Quantum Mechanics Molecular Mechanics
RAS	Restricted Active Spaces
RPA	Random Phase Approximation

Encyclopedia of Analytical Chemistry, Online © 2006–2013 John Wiley & Sons, Ltd.

This article was published in the *Encyclopedia of Analytical Chemistry* in 2013 by John Wiley & Sons, Ltd.
DOI: 10.1002/9780470027318.a6109.pub2

SCF	Self-consistent Field
SD	Spin Dipolar
SO	Spin Orbit
SOPPA	Second-order Polarization Propagator Approximation
SOS	Sum Over States
TMS	Tetramethylsilane
UHF	Unrestricted Hartree–Fock
ZORA	Zeroth-order Regular Approximation

RELATED ARTICLES

Nuclear Magnetic Resonance and Electron Spin Resonance Spectroscopy **(Volume 13)**
Chemical Shifts in Nuclear Magnetic Resonance

Nuclear Magnetic Resonance and Electron Spin Resonance Spectroscopy **(Volume 14)**
Quadrupole Couplings in Nuclear Magnetic Resonance, General • Scalar Couplings in Nuclear Magnetic Resonance, General

REFERENCES

1. N.F. Ramsey, 'Magnetic Shielding of Nuclei in Molecules', *Phys. Rev.*, **78**(6), 699–703 (1950).
2. N.F. Ramsey, 'Chemical Effects in Nuclear Magnetic Resonance and in Diamagnetic Susceptibility', *Phys. Rev.*, **86**(2), 243–246 (1952).
3. N.F. Ramsey, 'Electron Coupled Interactions Between Nuclear Spins in Molecules', *Phys. Rev.*, **91**(2), 303–307 (1953).
4. F. Michelot, 'Nuclear Hyperfine Interactions in Nonlinear Semi-Rigid Molecules I. The Molecular Hamiltonian', *Mol. Phys.*, **45**(5), 949–970 (1982).
5. F. Michelot, 'Nuclear Hyperfine Interactions in Nonlinear Semi-rigid Molecules II. The Effective Hamiltonian for a Non-degenerate Electronic State', *Mol. Phys.*, **45**(5), 971–1001 (1982).
6. M. Kaupp, M. Bühl, V.G. Malkin (eds), *Calculation of NMR and EPR Parameters. Theory and Applications*, Wiley-VCH, Weinheim, 2004.
7. A.E. Hansen, T.D. Bouman, 'Localized Orbital/Local Origin Method for Calculation and Analysis of NMR Shieldings. Applications to ^{13}C Shielding Tensors', *J. Chem. Phys.*, **82**(11), 5035–5047 (1985).
8. W. Kutzelnigg, U. Fleischer, M. Schindler, '*Ab Initio Calculation and Interpretation of Chemical Shifts in NMR by Means of the IGLO Method*', *NMR Basic Princ. Prog.*, **23**, 165–262 (1990).
9. K. Wolinski, J.F. Hinton, P. Pulay, 'Efficient Implementation of the Gauge-Independent Atomic Orbital Method for NMR Chemical Shift Calculations', *J. Am. Chem. Soc.*, **112**(23), 8251–8260 (1990).
10. T.A. Keith, R.F.W. Bader, 'Calculation of Magnetic Response Properties Using Atoms in Molecules', *Chem. Phys. Lett.*, **194**(1–2), 1–8 (1992).
11. P. Pyykkö, 'Relativistic Theory of Nuclear Spin–Spin Coupling in Molecules', *Chem. Phys.*, **22**, 289–296 (1977).
12. T. Helgaker, M. Jaszunski, K. Ruud, '*Ab Initio* Methods for the Calculation of NMR Shielding and Indirect Spin–Spin Coupling Constants', *Chem. Rev.*, **99**, 293–352 (1999).
13. K. Wolinski, C.L. Hsu, J.F. Hinton, P. Pulay, 'Hartree–Fock and 2nd Order Møller–Plesset Perturbation Theory Calculations of the ^{31}P NMR Shielding Tensor in PH_3', *J. Chem. Phys.*, **99**(10), 7819–7824 (1993).
14. G.D. Purvis, R.J. Bartlett, 'A Full Coupled Cluster Singles and Doubles Model: The Inclusion of Disconnected Triples', *J. Chem. Phys.*, **76**(4), 1910–1918 (1982).
15. J. Gauss, J.F. Stanton, 'Coupled Cluster Calculations of NMR Chemical Shifts', *J. Chem. Phys.*, **103**(9), 3561–3577 (1995).
16. J. Gauss, J.F. Stanton, 'Perturbative Treatment of Triple Excitations in Coupled Cluster Calculations of Nuclear Magnetic Shielding Constants', *J. Chem. Phys.*, **104**(7), 2574–2583 (1996).
17. A. Barszczewicz, T. Helgaker, M. Jaszunski, P. Jørgensen, K. Ruud, 'NMR Shielding Tensors and Indirect Spin–Spin Coupling Tensors in HCN, HNC, CH_3CN and CH_3NC Molecules', *J. Magn. Reson. A*, **114**(2), 212–218 (1995).
18. J. Gauss, K. Ruud, 'On the Convergence of MBPT and CC Nuclear Shielding Constants of BH Toward the Full CI Limit', *Int. J. Quantum Chem.*, **S29**, 437–442 (1995).
19. J. Geertsen, J. Oddershede, 'Second Order Polarization Propagator Calculations of Indirect Nuclear Spin–Spin Coupling Tensors in the Water Molecule', *Chem. Phys.*, **90**, 301–311 (1984).
20. J. Geertsen, J. Oddershede, W.T. Raynes, G.E. Scuseria, 'Nuclear Spin–Spin Coupling in the Methane Isotopomers', *J. Magn. Reson.*, **93**, 458–471 (1991).
21. S.A. Perera, H. Sekino, R.J. Bartlett, 'Coupled Cluster Calculations of Indirect Nuclear Coupling Constants: The Importance of Non-Fermi Contact Contributions', *J. Chem. Phys.*, **101**(3), 2186–2191 (1994).
22. S. Kirpekar, H.J. Aa, J.O. Jensen, 'Correlated Calculations of Indirect Nuclear Spin–Spin Coupling Constants for XH_4 (X = Si, Ge, and Sn)', *Chem. Phys.*, **188**(171–181), (1994).

Encyclopedia of Analytical Chemistry, Online © 2006–2013 John Wiley & Sons, Ltd.

This article was published in the *Encyclopedia of Analytical Chemistry* in 2013 by John Wiley & Sons, Ltd.
DOI: 10.1002/9780470027318.a6109.pub2

23. J.F. Stanton, J. Gauss, 'Analytic Second Derivatives in High-Order Many-Body Perturbation and Coupled-Cluster Theories: Computational Considerations and Applications', *Int. Rev. Phys. Chem.*, **19**, 61–95 (2000).
24. T. Helgaker, M. Jaszuński, P. Garbacz, K. Jackowski, 'The NMR Indirect Nuclear Spin–Spin Coupling Constant of the HD Molecule', *Mol. Phys.*, **110**, 2611–2617 (2012).
25. R.G. Parr, W. Yang, *Density Functional Theory of Atoms and Molecules*, Oxford University Press, Oxford, 1989.
26. G. Vignale, M. Rasolt, D.J.W. Geldart, 'Magnetic Fields and Density Functional Theory', *Adv. Quantum Chem.*, **21**, 235–253 (1990).
27. C.J. Grayce, R.A. Harris, 'Magnetic Field Density Functional Theory', *Phys. Rev. A*, **50**(4), 3089–3095 (1994).
28. C.J. Grayce, R.A. Harris, 'Two Dipole Magnetic Field Density Functional Theory', *J. Phys. Chem.*, **99**(9), 2724–2726 (1995).
29. A.M. Lee, N.C. Handy, S.M. Colwell, 'The Density Functional Calculation of Nuclear Shielding Constants Using London Atomic Orbitals', *J. Chem. Phys.*, **103**(23), 10095–10109 (1995).
30. A.D. Becke, 'Density Functional Thermochemistry. III. The Role of Exact Exchange', *J. Chem. Phys.*, **98**(7), 5648–5652 (1993).
31. C. Lee, W. Yang, R.G. Parr, 'Development of the Colle-Salvetti Correlation-Energy Formula into a Functional of the Electron Density', *Phys. Rev. B*, **37**(2), 785–789 (1988).
32. V.G. Malkin, O.L. Malkina, M.E. Casida, D.R. Salahub, 'NMR Shielding Tensors Calculated with a Sum over States Density Functional Perturbation Theory', *J. Am. Chem. Soc.*, **116**(13), 5898–5908 (1994).
33. G. Schreckenbach, T. Ziegler, 'Calculation of NMR Shielding Tensors Using Gauge-Including Atomic Orbitals and Modern Density Functional Theory', *J. Phys. Chem.*, **99**(2), 606–611 (1995).
34. G. Rauhut, S. Puryear, K. Wolinski, P. Pulay, 'Comparison of NMR Shieldings Calculated from Hartree–Fock and Density Functional Wavefunctions Using Gauge-Including Atomic Orbitals', *J. Phys. Chem.*, **100**(15), 6310–6316 (1996).
35. T.A. Keith, R.F.W. Bader, 'Calculation of Magnetic Response Properties Using a Continuous Set of Gauge Transformations', *Chem. Phys. Lett.*, **210**(1–3), 223–231 (1993).
36. A.M. Teale, O.B. Lutnæs, T. Helgaker, D.J. Tozer, J. Gauss, 'Benchmarking Density-Functional Theory Calculations of NMR Shielding Constants and Spin–Rotation Constants Using Accurate Coupled-Cluster Calculations', *J. Chem. Phys.*, **138**, 024111 (2013).
37. T. Helgaker, M. Watson, N.C. Handy, 'Analytical Calculation of Nuclear Magnetic Resonance Indirect Spin–Spin Coupling Constants at the Generalized Gradient Approximation and Hybrid Levels of Density-Functional Theory', *J. Chem. Phys.*, **113**, 9402–9409 (2000).
38. M.A. Watson, N.C. Handy, A.J. Cohen, T. Helgaker, 'Density-Functional Generalized-Gradient and Hybrid Calculations of Electromagnetic Properties Using Slater Basis Sets', *J. Chem. Phys.*, **120**, 7252–7261 (2004).
39. L. Visscher, T. Enevoldsen, T. Saue, H.J.A. Jensen, J. Oddershede, 'Full Four-Component Relativistic Calculations of NMR Shielding and Indirect Spin–Spin Coupling Tensors in Hydrogen Halides', *J. Comput. Chem.*, **20**, 1262–1273 (1999).
40. M. Kato, M. Hada, R. Fukuda, H. Nakatsuji, 'Relativistic Configuration Interaction and Coupled Cluster Methods Using Four-Component Spinors: Magnetic Shielding Constants of HX and CH_3X (X = F, Cl, Br, I)', *Chem. Phys. Lett.*, **408**, 150–156 (2005).
41. S. Komorovsky, M. Repisky, O.L. Malkina, V.G. Malkin, 'Fully Relativistic Calculations of NMR Shielding Tensors Using Restricted Magnetically Balanced Basis and Gauge Including Atomic Orbitals', *J. Chem. Phys.*, **132**, 154101 (2010).
42. M. Olejniczak, R. Bast, T. Saue, M. Pecul, 'A Simple Scheme for Magnetic Balance in Four-Component Relativistic Kohn–Sham Calculations of Nuclear Magnetic Resonance Shielding Constants in a Gaussian Basis', *J. Chem. Phys.*, **136**, 014108 (2012).
43. Q. Sun, Y. Xiao, W. Liu, 'Exact Two-Component Relativistic Theory for NMR Parameters: General Formulation and Pilot Application', *J. Chem. Phys.*, **137**, 174105 (2012).
44. J. Autschbach, D. Peng, M. Reiher, 'Two-Component Relativistic Calculations of Electric-Field Gradients Using Exact Decoupling Methods: Spin–Orbit and Picture-Change Effects', *J. Chem. Theory Comput.*, **8**, 4239–4248 (2012).
45. C.J. Jameson, J. Mason, '*The Chemical Shift*', in *Multinuclear NMR*, ed. J. Mason, Plenum, New York, 51–88, 1987.
46. H. Takashima, M. Hada, H. Nakatsuji, 'Spin–Orbit Effect on the Magnetic Shielding Constant Using the *Ab Initio* UHF Method – Ga and In Tetrahalides', *Chem. Phys. Lett.*, **235**(1–2), 13–16 (1995).
47. G.A. Aucar, J. Oddershede, 'Relativistic Theory for Indirect Nuclear Spin–Spin Couplings Within the Polarization Propagator Approach', *Int. J. Quantum Chem.*, **47**, 425–435 (1993).
48. J.I. Melo, M.C. Ruiz de Azúa, J.E. Peralta, G.E. Scuseria, 'Relativistic Calculation of Indirect NMR Spin–Spin Couplings Using the Douglas–Kroll–Hess Approximation', *J. Chem. Phys.*, **123**, 204112 (2005).

Encyclopedia of Analytical Chemistry, Online © 2006–2013 John Wiley & Sons, Ltd.

This article was published in the *Encyclopedia of Analytical Chemistry* in 2013 by John Wiley & Sons, Ltd.
DOI: 10.1002/9780470027318.a6109.pub2

49. P. Pyykkö, J.R. Wiesenfeld, 'Relativistically Parameterized Extended Hückel Calculations IV. Nuclear Spin–Spin Coupling Tensors for Main Group Elements', *Mol. Phys.*, **43**(3), 557–580 (1981).
50. V. Arcisauskaite, S. Knecht, S.P.A. Sauer, L. Hemmingsen, 'Fully Relativistic Coupled Cluster and DFT Study of Electric Field Gradients at Hg in ^{199}Hg Compounds', *Phys. Chem. Chem. Phys.*, **14**, 2651–2657 (2012).
51. J. Autschbach, 'Perspective: Relativistic Effects', *J. Chem. Phys.*, **136**, 150902 (2012).
52. J. Autschbach, S. Zheng, 'Relativistic Computations of NMR Parameters from First Principles: Theory and Applications', *Annu. Rep. NMR Spectrosc.*, **67**, 1–95 (2009).
53. W. Kutzelnigg, W.J. Liu, 'Relativistic Theory of Nuclear Magnetic Resonance Parameters in a Gaussian Basis Representation', *J. Chem. Phys.*, **131**, 044129 (2009).
54. S.A. Joyce, J.R. Yates, C.J. Pickard, S.P. Brown, 'Density Functional Theory Calculations of Hydrogen-Bond-Mediated NMR J Coupling in the Solid State', *J. Am. Chem. Soc.*, **130**, 12663–70 (2008).
55. F. Mauri, B. Pfrommer, S.G. Louie, 'Ab-Initio Theory of NMR Chemical Shifts in Solids and Liquids', *Phys. Rev. Lett.*, **77**, 5300–5303 (1996).
56. A.C. de Dios, C.J. Jameson, 'Recent Advances in Nuclear Shielding Calculations', *Annu. Rep. NMR Spectrosc.*, **77**, 1–80 (2012).
57. C.J. Pickard, F. Mauri, 'All-Electron Magnetic Response with Pseudopotentials: NMR Chemical Shifts', *Phys. Rev. B*, **63**, 245101 (2001).
58. J.R. Yates, C.J. Pickard, F. Mauri, 'Calculation of NMR Chemical Shifts for Extended Systems Using Ultrasoft Pseudopotentials', *Phys. Rev. B*, **76**, 024401 (2007).
59. J.R. Yates, C.J. Pickard, M.C. Payne, F. Mauri, 'Relativistic Nuclear Magnetic Resonance Chemical Shifts of Heavy Nuclei with Pseudopotentials and the Zeroth-Order Regular Approximation', *J. Chem. Phys.*, **118**, 5746–5743 (2003).
60. S.A. Joyce, J.R. Yates, C.J. Pickard, F. Mauri, 'A First Principles Theory of Nuclear Magnetic Resonance J-Coupling in Solid-State Systems', *J. Chem. Phys.*, **127**, 204107 (2007).
61. J.R. Yates, C.J. Pickard, 'Computations of Magnetic Resonance Parameters for Crystalline Systems: Principles', in *Encyclopedia of Magnetic Resonance*, eds R.K. Harris, R.E. Wasylishen, John Wiley & Sons, Chichester, 2008. DOI: 10.1002/9780470034590.emrstm1009
62. J.R. Yates, 'Prediction of NMR J-Coupling in Solids with the Planewave Pseudopotential Approach', *Magn. Reson. Chem.*, **48**, S23–S31 (2010).
63. W. Keal, D.J. Tozer, 'The Exchange-Correlation Potential in Kohn–Sham Nuclear Magnetic Resonance Shielding Calculations', *J. Chem. Phys.*, **119**, 3015–3024 (2003).
64. J. Gauss, 'GIAO-MBPT(3) and GIAO-SDQ-MBPT(4) Calculations of NMR Shielding Constants', *Chem. Phys. Lett.*, **229**(3), 198–203 (1994).
65. K. Ruud, T. Helgaker, R. Kobayashi, P. Jørgensen, K.L. Bak, H.J.A. Jensen, 'Multiconfigurational Self Consistent Field Calculations of Nuclear Shieldings Using London Atomic Orbitals', *J. Chem. Phys.*, **100**(11), 8178–8185 (1994).
66. J. Gauss, 'Accurate Calculation of NMR Chemical Shifts', *Ber. Bunsenges. Phys. Chem.*, **99**(8), 1001–1008 (1995).
67. J. Gauss, 'Effects of Electron Correlation in the Calculation of Nuclear Magnetic Resonance Chemical Shifts', *J. Chem. Phys.*, **99**(5), 3629–3643 (1993).
68. A.K. Jameson, C.J. Jameson, 'Gas Phase ^{13}C Chemical Shifts in the Zero-Pressure Limit. Refinements to the Absolute Shielding Scale for ^{13}C', *Chem. Phys. Lett.*, **134**(5), 461–466 (1987).
69. D.M. Grant, J.C. Facelli, D.W. Alderman, M.H. Sherwood, '*Carbon-13 Chemical Shielding Tensors in Sugars: Sucrose and Methyl-(–D-Glucopyranoside)*', in *Nuclear Magnetic Shielding and Molecular Structure*, ed. J.A. Tossell, Kluwer Academic, Dordrecht, 367–384, 1993.
70. F. Liu, C.G. Phung, D.W. Alderman, D.M. Grant, 'Carbon-13 Chemical Shift Tensors in Methyl Glycosides, Comparing Diffraction and Optimized Structures with Single-Crystal NMR', *J. Am. Chem. Soc.*, **118**(43), 10629–10634 (1996).
71. J.C. Facelli, D.M. Grant, 'Determination of Molecular Symmetry in Crystalline Naphthalene Using Solid State NMR', *Nature*, **365**, 325–327 (1993).
72. A.C. de Dios, D.D. Laws, E. Oldfield, 'Predicting ^{13}C NMR Chemical Shielding Tensors in Zwitterionic L-Threonine and L-Tyrosine via Quantum Chemistry', *J. Am. Chem. Soc.*, **116**(17), 7784–7786 (1994).
73. E. Prochnow, A.A. Auer, 'Quantitative Prediction of gas-Phase ^{15}N and ^{31}P Nuclear Magnetic Shielding Constants', *J. Chem. Phys.*, **132**, 064109 (2010).
74. A.A. Auer, 'Quantitative Prediction of Gas-Phase ^{17}O Nuclear Magnetic Shielding Constants', *J. Chem. Phys.*, **131**, 024116 (2009).
75. M.E. Harding, M. Lenhart, A.A. Auer, J. Gauss, 'Quantitative Prediction of Gas-Phase ^{19}F Nuclear Magnetic Shielding Constants', *J. Chem. Phys.*, **128**, 244111 (2008).
76. M. Kaupp, O.L. Malkina, V.G. Malkin, 'The Calculation of ^{17}O Chemical Shielding in Transition Metal Oxo Complexes. I. Comparison of DFT and *Ab Initio* Approaches, and Mechanisms of Relativity-Induced Shielding', *J. Chem. Phys.*, **106**(22), 9201–9212 (1997).
77. Y. Ruiz-Morales, G. Schreckenbach, T. Ziegler, 'Theoretical Study of ^{13}C and ^{17}O NMR Shielding Tensors in Transition Metal Carbonyl Based on Density Functional

Encyclopedia of Analytical Chemistry, Online © 2006–2013 John Wiley & Sons, Ltd.

This article was published in the *Encyclopedia of Analytical Chemistry* in 2013 by John Wiley & Sons, Ltd.
DOI: 10.1002/9780470027318.a6109.pub2

Theory and Gauge Including Atomic Orbitals', *J. Phys. Chem.*, **100**(9), 3359–3367 (1996).

78. D.B. Chesnut, E.F.C. Byrd, 'The Inclusion of Correlation in the Calculation of Phosphorus NMR Chemical Shieldings', *Heteroatom Chem.*, **7**(5), 307–312 (1996).
79. D.B. Chesnut, L.D. Quin, '^{33}S NMR Shieldings and Chemical Bonding in Compounds of Sulfur', *Heteroatom Chem.*, **15**, 216–224 (2004).
80. M.A. Fedotov, O.L. Malkina, V.G. Malkin, '$^{35/37}$Cl NMR Chemical Shifts and Nuclear Quadrupole Couplings for some Small Chlorine Compounds: Experimental and Theoretical Study', *Chem. Phys. Lett.*, **258**, 330–335 (1996).
81. R.P. Chapman, D.L. Bryce, 'Application of Multinuclear Magnetic Resonance and Gauge-Including Projector-Augmented-Wave Calculations to the Study of Solid Group 13 Chlorides', *Phys. Chem. Chem. Phys.*, **11**, 6987–6998 (2009).
82. C.J. Jameson, A.K. Jameson, 'Concurrent ^{19}F and ^{77}Se or ^{19}F and ^{125}Te NMR T_1 Measurements for Determination of ^{77}Se and ^{125}Te Absolute Shielding Scales', *Chem. Phys. Lett.*, **135**(3), 254–259 (1987).
83. M. Bühl, J. Gauss, J.F. Stanton, 'Accurate Computations of ^{77}Se NMR Chemical Shifts Using the GIAO-CCSD Method', *Chem. Phys. Lett.*, **241**(3), 248–252 (1995).
84. G. Schreckenbach, Y. Ruiz-Morales, T. Ziegler, 'The Calculation of ^{77}Se Chemical Shifts Using Gauge-Including Atomic Orbitals and Density Functional Theory', *J. Chem. Phys.*, **104**(21), 8605–8612 (1996).
85. C.J. Jameson, '*Theoretical and Physical Aspects of Nuclear Shielding*', in *Nuclear Magnetic Resonance*, ed. G.A. Webb, Royal Society of Chemistry, London, 39–82, Vol. **25**, 1996.
86. Y. Ruiz-Morales, G. Schreckenbach, T. Ziegler, 'Calculation of ^{125}Te Chemical Shifts Using Gauge Including Atomic Orbitals and Density Functional Theory', *J. Phys. Chem.*, **101**(22), 4121–4127 (1997).
87. R. Fukuda, H. Nakatsuji, 'Quasirelativistic Theory for the Magnetic Shielding Constant. III. Quasirelativistic Second-Order Møller–Plesset Perturbation Theory and its Application to Tellurium Compounds', *J. Chem. Phys.*, **123**, 044101 (2005).
88. P.D. Ellis, J.D. Odom, A.S. Lipton, Q. Chen, J.M. Gulick, '*Gas Phase Measurements and Ab Initio Calculations of ^{77}Se and ^{113}Cd Chemical Shifts*', in *Nuclear Magnetic Shielding and Molecular Structure*, ed. J.A. Tossell, Kluwer Academic, Dordrecht, 539–555, 1993.
89. T. Higashioji, M. Hada, M. Sugimoto, H. Nakatsuji, 'Basis Set Dependence of Magnetic Shielding Constant Calculated by the Hartree–Fock/Finite Perturbation Method', *Chem. Phys.*, **203**, 159–175 (1996).
90. O. Vahtras, H. Agren, P. Jørgensen, T. Helgaker, H.J.A. Jensen, 'The Nuclear Spin–Spin Coupling in N_2 and CO', *Chem. Phys. Lett.*, **209**(3), 201–206 (1993).
91. A.A. Auer, J. Gauss, 'Triple Excitation Effects in Coupled-Cluster Calculations of Indirect Spin–Spin Coupling Constants', *J. Chem. Phys.*, **115**, 1619–1622 (2001).
92. T. Helgaker, M. Jaszuński, M. Pecul, 'The Quantum-Chemical Calculation of NMR Indirect Spin–Spin Coupling Constants', *Prog. Nucl. Magn. Reson.*, **53**, 249–268 (2008).
93. J. Geertsen, J. Oddershede, G.E. Scuseria, 'Calculation of Spectra and Spin–Spin Coupling Constants Using a Coupled Cluster Polarization Propagator Method', *Int. J. Quantum Chem. Symp.*, **21**, 475–485 (1987).
94. H. Fukui, K. Miura, H. Matsuda, T. Baba, 'Calculation of Nuclear Spin–Spin Couplings. VII. Electron Correlation Effects on the Five Coupling Mechanisms', *J. Chem. Phys.*, **97**(4), 2299–2304 (1992).
95. V.G. Malkin, O.L. Malkina, D.R. Salahub, 'Calculations of Spin–Spin Coupling Constants Using Density Functional Theory', *Chem. Phys. Lett.*, **221**(1–2), 91–99 (1994).
96. J. Geertsen, J. Oddershede, G.E. Scuseria, 'Spin–Spin Coupling Constants of CO and N_2', *J. Chem. Phys.*, **87**(4), 2138–2142 (1987).
97. C.J. Jameson, J. Mason, '*Spin–Spin Coupling*', in *Multinuclear NMR*, ed. J. Mason, Plenum, New York, 89–132, 1987.
98. M.D. Lumsden, K. Eichele, R.E. Wasylishen, T.S. Cameron, J.F. Britten, 'Determination of a ^{199}Hg^{31}P Indirect Spin–Spin Coupling Tensor via Single-Crystal Phosphorus NMR Spectroscopy', *J. Am. Chem. Soc.*, **116**(24), 11129–11136 (1994).
99. D.L. Bryce, R.E. Wasylishen, 'Indirect Nuclear Spin–Spin Coupling Tensors in Diatomic Molecules: A Comparison of Results Obtained by Experiment and First Principles Calculations', *J. Am. Chem. Soc.*, **122**, 3197–3205 (2000).
100. M. Karplus, 'Contact Electron Spin Coupling of Nuclear Magnetic Moments', *J. Chem. Phys.*, **30**(1), 11–15 (1959).
101. H. Fukui, H. Inomata, T. Baba, K. Miura, H. Matsuda, 'Calculation of Nuclear Spin–Spin Couplings. VIII. Vicinal Proton–Proton Coupling Constants in Ethane', *J. Chem. Phys.*, **103**(15), 6597–6600 (1995).
102. M. Habeck, W. Rieping, M. Nilges, 'Bayesian Estimation of Karplus Parameters and Torsion Angles from Three-Bond Scalar Couplings Constants', *J. Magn. Reson.*, **177**, 160–165 (2005).
103. G. Breit, 'Possible Effects of Nuclear Spin on X-Ray Terms', *Phys. Rev.*, **35**(12), 1447–1451 (1930).
104. P. Pyykkö, E. Pajanne, M. Inokuti, 'Hydrogen-Like Relativistic Corrections for Electric and Magnetic

DOI: 10.1002/9780470027318.a6109.pub2

Hyperfine Integrals', *Int. J. Quantum Chem.*, **7**, 785–806 (1973).

105. D.L. Bryce, J. Autschbach, 'Relativistic Hybrid DFT Calculation of Indirect Nuclear Spin–Spin Coupling Tensors – Comparison with Experiment for Diatomic Alkali Metal Halides', *Can. J. Chem.*, **87**, 927–941 (2009).
106. R. Ludwig, F. Weinhold, T.C. Farrar, 'Experimental and Theoretical Studies of Hydrogen Bonding in Neat, Liquid Formamide', *J. Chem. Phys.*, **102**(13), 5118–5125 (1995).
107. B.F. King, T.C. Farrar, F. Weinhold, 'Quadrupole Coupling Constants in Linear $(HCN)_n$ Clusters: Theoretical and Experimental Evidence for Cooperativity Effects in C–H···N Hydrogen Bonding', *J. Chem. Phys.*, **103**(1), 348–352 (1995).
108. K.E. Vermillion, P. Florian, P.J. Grandinetti, 'Relationships Between Bridging Oxygen ^{17}O Quadrupolar Coupling Parameters and Structure in Alkali Silicates', *J. Chem. Phys.*, **108**(17), 7274–7285 (1998).
109. T.M. Clark, P.J. Grandinetti, '*The Structure of Oxide Glasses: Insights from ^{17}O NMR*', in *Modern Magnetic Resonance Part III*, ed. G.A. Webb, Springer, Dordrecht, 1543–1548, 2006.
110. J. Cuny, S. Messaoudi, V. Alonzo, E. Furet, J.-F. Halet, E. Le Fur, S.E. Ashbrook, C.J. Pickard, R. Gautier, L. Le Polles, 'DFT Calculations of Quadrupolar Solid-State NMR Properties: Some Examples in Solid-State Inorganic Chemistry', *J. Comput. Chem.*, **29**, 2279–2287 (2008).
111. L.A. Odell, R.W. Schurko, 'Static Solid-State ^{14}N NMR and Computational Studies of Nitrogen EFG Tensors in some Crystalline Amino Acids', *Phys. Chem. Chem. Phys.*, **11**, 7069–7077 (2009).
112. J. Autschbach, S. Zheng, R.W. Schurko, 'Analysis of Electric Field Gradient Tensors at Quadrupolar Nuclei in Common Structural Motifs', *Concepts Magn. Reson. A*, **36**, 84–126 (2010).
113. L. Visscher, T. Enevoldsen, T. Saue, J. Oddershede, 'Molecular Relativistic Calculations of the Electric Field Gradients at the Nuclei in the Hydrogen Halides', *J. Chem. Phys.*, **109**, 9677–9684 (1998).
114. M. Filatov, W. Zou, D. Cremer, 'Relativistically Corrected Electric Field Gradients Calculated with the Normalized Elimination of the Small Component Formalism', *J. Chem. Phys.*, **137**, 054113 (2012).
115. C.M. Widdifield, D.L. Bryce, 'Solid-State 127I NMR and GIPAW DFT Study of Metal Iodides and Their Hydrates: Structure, Symmetry, and Higher-Order Quadrupole-Induced Effects', *J. Phys. Chem. A*, **114**, 10810–10823 (2010).
116. A.C. de Dios, C.J. Jameson, 'The NMR Chemical Shift: Insight into Structure and Environment', *Annu. Rep. NMR Spectrosc.*, **29**, 1–69 (1994).
117. A.C. de Dios, J.G. Pearson, E. Oldfield, 'Secondary and Tertiary Structural Effects on Protein NMR Chemical Shifts: An *Ab Initio* Approach', *Science*, **260**, 1491–1496 (1993).
118. A.C. de Dios, E. Oldfield, '*Ab Initio* Study of the Effects of Torsion Angles on Carbon-13 Nuclear Magnetic Resonance Chemical Shielding in N-Formyl-L-Alanine, N-Formyl-L-Valine Amide, and Some Simple Model Compounds: Applications to Protein NMR Spectroscopy', *J. Am. Chem. Soc.*, **116**(12), 5307–5314 (1994).
119. H.B. Le, J.G. Pearson, A.C. de Dios, E. Oldfield, 'Protein Structure Refinement and Prediction via NMR Chemical Shifts and Quantum Chemistry', *J. Am. Chem. Soc.*, **117**(13), 3800–3807 (1995).
120. C.J. Jameson, A.C. de Dios, '*The Nuclear Shielding Surface: The Shielding as a Function of Molecular Geometry and Intermolecular Separation*', in *Nuclear Magnetic Shielding and Molecular Structure*, ed. J.A. Tossell, Kluwer Academic, Dordrecht, 95–116, 1993.
121. C.J. Jameson, 'Understanding NMR Chemical Shifts', *Ann. Rev. Phys. Chem.*, **47**, 135–169 (1996).
122. Y. Shen, O. Lange, F. Delaglio, P. Rossi, J.M. Aramini, G. Liu, A. Eletsky, Y. Wu, K.K. Singarapu, A. Lemak, A. Ignatchenko, C.H. Arrowsmith, T. Szyperski, G.T. Montelione, D. Baker, A. Bax, 'Consistent Blind Protein Structure Generation from NMR Chemical Shift Data', *Proc. Natl. Acad. Sci. U. S. A.*, **105**, 4685–4690 (2008).
123. D.S. Wishart, D. Arndt, M. Berjanskii, P. Tang, J. Zhou, G. Lin, 'CS23D a Web Server for Rapid Protein Structure Generation Using NMR Chemical Shifts and Sequence Data', *Nucleic Acids Res.*, **36**, W496–502 (2008).
124. M. Berjanskii, P. Tang, J. Liang, J.A. Cruz, J.J. Zhou, Y. Zhou, E. Bassett, C. MacDonell, P. Lu, G.H. Lin, D.S. Wishart, 'GeNMR a Web Server for Rapid NMR-Based Protein Structure Determination', *Nucleic Acids Res.*, **37**, W670–W677 (2009).
125. C.J. Jameson, '*Rovibrational Averaging of Molecular Electronic Properties*', in *Theoretical Models of Chemical Bonding, Part 3. Molecular Spectroscopy, Electronic Structure, and Intramolecular Interactions*, ed. Z.B. Maksic, Springer-Verlag, Berlin, 457–519, 1991.
126. W.T. Raynes, J. Geertsen, J. Oddershede, 'Nuclear Spin–Spin Coupling and Nuclear Motion', *Int. J. Quantum Chem.*, **52**(1), 153–163 (1994).
127. K. Sneskov, J.F. Stanton, 'Effects of Vibrational Averaging on Coupled Cluster Calculations of Spin–Spin Coupling Constants for Hydrocarbons', *Mol. Phys.*, **110**, 2321–2327 (2012).
128. A. Yachmenev, S.N. Yurchenko, I. Paidarova, P. Jensen, W. Thiel, S.P.A. Sauer, 'Thermal Averaging of the Indirect Nuclear Spin–Spin Coupling Constants of

Encyclopedia of Analytical Chemistry, Online © 2006–2013 John Wiley & Sons, Ltd.

This article was published in the *Encyclopedia of Analytical Chemistry* in 2013 by John Wiley & Sons, Ltd.
DOI: 10.1002/9780470027318.a6109.pub2

Ammonia: The Importance of the Large Amplitude Inversion Mode', *J. Chem. Phys.*, **132**, 114305 (2010).

129. J.F. Hinton, P. Guthrie, P. Pulay, K. Wolinski, '*Ab Initio* Quantum Mechanical Calculation of the Chemical Shift Anisotropy of the Hydrogen Atom in the $(H_2O)_{17}$ Cluster', *J. Am. Chem. Soc.*, **114**(5), 1604–1605 (1992).
130. P.B. Karadakov, K. Morokuma, 'ONIOM as an Efficient Tool for Calculating NMR Chemical Shielding Constants in Large Molecules', *Chem. Phys. Lett.*, **317**, 589–596 (2000).
131. Q. Cui, M. Karplus, 'Molecular Properties from Combined QM/MM Methods. 2. Chemical Shifts in Large Molecules', *J. Phys. Chem. B*, **104**, 3721–3743 (2000).
132. D.F. Stueber, 'The Embedded Ion Method: A New Approach to the Electrostatic Description of Crystal Lattice Effects in Chemical Shielding Calculations', *Concepts Magn. Reson. A*, **28**, 347–368 (2006).
133. T.B. Woolf, V.G. Malkin, O.L. Malkina, D.R. Salahub, B. Roux, 'The Backbone ^{15}N Chemical Shift Tensor of the Gramicidin Channel. A Molecular Dynamics and Density Functional Study', *Chem. Phys. Lett.*, **239**, 186–194 (1995).
134. C.J. Jameson, A.K. Jameson, B.I. Baello, H.M. Lim, 'Grand Canonical Monte Carlo Simulations of Xenon in Zeolite NaA, I. Distribution and ^{129}Xe Chemical Shifts', *J. Chem. Phys.*, **100**(8), 5965–5976 (1994).
135. C.J. Jameson, A.K. Jameson, R.E. Gerald II,, H.M. Lim, 'Anisotropic Xe Chemical Shifts in Zeolites. The Role of Intra- and Inter-Crystallite Diffusion', *J. Phys. Chem.*, **101**(42), 8418–8437 (1997).
136. R.M. Gester, H.C. Georg, S. Canuto, M.C. Caputo, P.F. Provasi, 'NMR Chemical Shielding and Spin–Spin Coupling Constants of Liquid NH_3: A Systematic Investigation Using the Sequential QM/MM Method', *J. Phys. Chem. A*, **113**, 14936–14942 (2009).
137. C. Bonhomme, C. Gervais, F. Babonneau, C. Coelho, F. Pourpoint, T. Azaïs, S.E. Ashbrook, J.M. Griffin, J.R. Yates, F. Mauri, C.J. Pickard, 'First-Principles Calculation of NMR Parameters Using the Gauge-Including Projector Augmented Wave Method: A Chemist's Point of View', *Chem. Rev.*, **112**, 5733–5779 (2012).

Encyclopedia of Analytical Chemistry, Online © 2006–2013 John Wiley & Sons, Ltd.

This article was published in the *Encyclopedia of Analytical Chemistry* in 2013 by John Wiley & Sons, Ltd.
DOI: 10.1002/9780470027318.a6109.pub2